

① LEVEL II

CM-CCM-79-3

October 1979

ADA 080979

Interception of Hostile Communications

DDC FILE COPY

By Don J. Torrieri

DTIC ELECTE  
S FEB 20 1980 D  
B



U.S. Army Materiel Development  
and Readiness Command  
Countermeasures/  
Counter-countermeasures Office  
2800 Powder Mill Road  
Adelphi, MD 20783

Approved for public release; distribution unlimited.

80 2 19 223

The findings in this report are not to be construed as an official Department of the Army position unless so designated by other authorized documents.

Citation of manufacturers' or trade names does not constitute an official indorsement or approval of the use thereof.

Destroy this report when it is no longer needed. Do not return it to the originator.



*Editorial review and camera-ready copy by Technical Reports Branch,  
Harry Diamond Laboratories*

UNCLASSIFIED

SECURITY CLASSIFICATION OF THIS PAGE (When Data Entered)

REPORT DOCUMENTATION PAGE		READ INSTRUCTIONS BEFORE COMPLETING FORM	
1. REPORT NUMBER 14 CM-CCM-79-3	2. GOVT ACCESSION NO.	3. RECIPIENT'S CATALOG NUMBER	
4. TITLE (and Subtitle) 6 Interception of Hostile Communications.		5. TYPE OF REPORT & PERIOD COVERED 9 Technical Report	
7. AUTHOR(s) 10 Don J. Torrieri		6. PERFORMING ORG. REPORT NUMBER	
9. PERFORMING ORGANIZATION NAME AND ADDRESS Countermeasures/Counter-countermeasures Office, 2800 Powder Mill Road Adelphi, MD 20783		8. CONTRACT OR GRANT NUMBER(s)	
11. CONTROLLING OFFICE NAME AND ADDRESS U.S. Army Materiel Development & Readiness Command Alexandria, VA 22333		10. PROGRAM ELEMENT, PROJECT, TASK AREA & WORK UNIT NUMBERS Program Ele: 6.37.49.A DA: 1S463749D462	
14. MONITORING AGENCY NAME & ADDRESS (if different from Controlling Office)		12. REPORT DATE 11 October 1979	
		13. NUMBER OF PAGES 70	12 72
		15. SECURITY CLASS. (of this report) Unclassified	
		15a. DECLASSIFICATION/DOWNGRADING SCHEDULE	
16. DISTRIBUTION STATEMENT (of this Report) Approved for public release; distribution unlimited.			
17. DISTRIBUTION STATEMENT (of the abstract entered in Block 20, if different from Report)			
18. SUPPLEMENTARY NOTES ERADCOM Project: T499TA DRCMS Code: 643749.4620011			
19. KEY WORDS (Continue on reverse side if necessary and identify by block number) Interception                      Microscan receiver Radiometer                        Frequency estimation Direction finding                Countermeasures Detection                           Interferometer Cross correlation			
20. ABSTRACT (Continue on reverse side if necessary and identify by block number) Whatever the ultimate purpose of an interception system is, it nearly always must achieve the three basic functions of detection, frequency estimation, and direction finding. The fundamental concepts and issues of these three elements of interception are presented at the systems level, assuming that little is known about the signals to be intercepted. The capabilities of radiometers and cross correlators for detection are determined. Channelized,			

DD FORM 1 JAN 73 1473 EDITION OF 1 NOV 65 IS OBSOLETE

UNCLASSIFIED

SECURITY CLASSIFICATION OF THIS PAGE (When Data Entered)

410947

lpg

UNCLASSIFIED

SECURITY CLASSIFICATION OF THIS PAGE(When Data Entered)

Item 20 Cont'd.

discrete Fourier transform, acousto-optical, instantaneous frequency measurement, scanning superheterodyne, and microscan receivers for frequency estimation are described and analyzed. Direction finding by energy comparison systems with radiometers is analyzed. The two types of interferometers are discussed.

ACCESSION for	
NTIS	White Section <input checked="" type="checkbox"/>
DDC	Buff Section <input type="checkbox"/>
UNANNOUNCED	<input type="checkbox"/>
JUSTIFICATION	
BY	
DISTRIBUTION/AVAILABILITY CODES	
Dist.	AVAIL. and/or SPECIAL
A	

UNCLASSIFIED

SECURITY CLASSIFICATION OF THIS PAGE(When Data Entered)

CONTENTS

	<u>Page</u>
1. INTRODUCTION . . . . .	5
2. DETECTION . . . . .	5
2.1 Radiometer . . . . .	8
2.2 Channelized Radiometer . . . . .	15
2.3 Cross Correlator . . . . .	19
3. FREQUENCY ESTIMATION . . . . .	26
3.1 Channelized Receiver . . . . .	26
3.2 Spectrum Analysis with Discrete Fourier Transform . . . . .	28
3.3 Acousto-optical Receiver . . . . .	31
3.4 Instantaneous Frequency Measurement . . . . .	33
3.5 Scanning Superheterodyne Receiver . . . . .	35
3.6 Microscan Receiver . . . . .	41
4. DIRECTION FINDING . . . . .	47
4.1 Energy Comparison Systems . . . . .	47
4.2 Interferometer . . . . .	56
5. CONCLUSIONS . . . . .	60
LITERATURE CITED . . . . .	63
GLOSSARY OF PRINCIPAL SYMBOLS . . . . .	65
DISTRIBUTION . . . . .	69

FIGURES

1 Correlation detector . . . . .	6
2 Optimum detector for pulsed sinusoid of unknown frequency . . . . .	7
3 Radiometer . . . . .	8
4 Channelized radiometers . . . . .	15
5 Cross correlator . . . . .	20
6 Channelized receiver with filters arranged in successive stages . . . . .	28
7 Acousto-optical spectrum analyzer . . . . .	32

Figures (Cont'd)

	<u>Page</u>
8 Acousto-optical diffraction geometry for input at single frequency . . . . .	32
9 Array of Bragg cells for simultaneous frequency estimation and direction finding . . . . .	34
10 Instantaneous frequency measurement receiver . . . . .	34
11 Scanning superheterodyne receiver . . . . .	36
12 Time-frequency diagram for scanning superheterodyne receiver . . . . .	37
13 Microscan receivers . . . . .	41
14 Response of scanning superheterodyne and microscan receivers to simultaneous signals . . . . .	44
15 Stationary multibeam system . . . . .	48
16 Adjacent antenna radiation patterns . . . . .	48
17 Root-mean-square error versus arrival angle for different beam widths . . . . .	52
18 Root-mean-square error versus arrival angle for optimal beam widths and different values of $\gamma$ . . . . .	52
19 Rotating beam system . . . . .	53
20 Rotating monopulse system . . . . .	54
21 Interferometers . . . . .	57

## 1. INTRODUCTION

Interception of hostile communications is attempted for many diverse reasons, such as reconnaissance, surveillance, position fixing, identification, or a prelude to jamming. Different purposes require different systems, but whatever the purpose, an interception system nearly always must achieve the three basic functions of detection, frequency estimation, and direction finding. Although these three elements of interception are usually integrated in a practical system, they are discussed separately in this paper for clarity of presentation. The basic concepts and issues of the three elements are presented at the systems level, assuming that little is known about the signals to be intercepted. Primarily because of the rapidly changing technological base, the implementation and the engineering details of the interception systems are not addressed. Although this paper is concerned with the interception of communications, only slight modifications of the results are required to apply them to the interception of radar.

The potential interceptor has at least one major advantage over the communicators. The accuracies of detection, frequency estimation, and direction finding are determined by the energy of the entire message transmitted, which may include many symbols. In contrast, the intended receiver makes decisions with accuracies determined by the energy of each transmitted symbol. From another point of view, the intended receiver generally must make many separate decisions, whereas the interception receiver must make only a few decisions.

## 2. DETECTION

If the form and the parameters of the signal to be intercepted,  $s(t)$ , were known, optimum detection in white Gaussian noise,  $n(t)$ , could be accomplished by a matched filter or an ideal correlator. Figure 1 depicts a correlator for the received signal,  $r(t) = s(t) + n(t)$ , and an observation interval,  $T$ . The comparator input is compared with a fixed threshold level,  $V_T$ , to determine the presence of an intercepted signal. It is a standard result that the probability of false alarm,  $P_F$ , and the probability of detection,  $P_D$ , are given by<sup>1</sup>

$$P_F = \frac{1}{2} \operatorname{erfc} \left[ \frac{V_T}{(N_0 E)^{1/2}} \right], \quad (1)$$

$$P_D = \frac{1}{2} \operatorname{erfc} \left[ \frac{V_T}{(N_0 E)^{1/2}} - \left( \frac{E}{N_0} \right)^{1/2} \right], \quad (2)$$

<sup>1</sup>A. Whalen, *Detection of Signals in Noise*, Academic Press, Inc., New York (1971).

where  $E$  is the signal energy,  $N_0/2$  is the noise power spectral density, and the complementary error function is defined as

$$\operatorname{erfc}(x) = \frac{2}{\sqrt{\pi}} \int_x^{\infty} \exp(-v^2) dv . \quad (3)$$

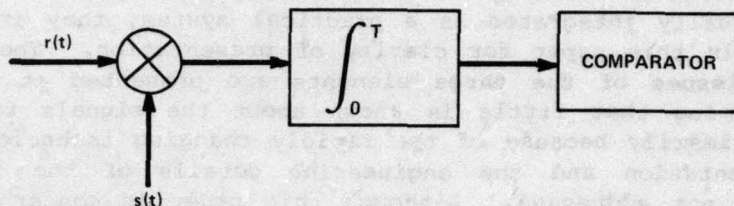


Figure 1. Correlation detector.

Denoting the inverse complementary error function by  $\operatorname{erfc}^{-1}$ , we define

$$\beta = \operatorname{erfc}^{-1}(2P_F) , \quad (4)$$

$$\xi = \operatorname{erfc}^{-1}(2P_D) . \quad (5)$$

From equations (1) and (2), we can calculate the value of  $E/N_0$  necessary to ensure specified  $P_F$  and  $P_D$ . The result is

$$\frac{E}{N_0} = (\beta - \xi)^2 . \quad (6)$$

Although the ideal correlator cannot be used when  $s(t)$  is unknown, equation (6) provides a basis of comparison for more realistic interception receivers.

To detect the presence of an unknown signal, we assume that the intercepted signal has random phase and frequency and an unknown constant amplitude. The signal frequency is assumed to be one of  $M$  possible values; that is, the band to be searched is divided into  $M$  channels with center frequencies  $\omega_1, \omega_2$ , etc. To each discrete frequency,  $\omega_i$ , we assign a hypothesis,  $H_i$ . Thus, the multiple alternative hypotheses over an observation interval are



$$H_0: r(t) = n(t), \quad 0 \leq t \leq T,$$

$$H_1: r(t) = A \sin(\omega_1 t + \theta_1) + n(t), \quad 0 \leq t \leq T,$$

.

.

.

$$H_M: r(t) = A \sin(\omega_M t + \theta_M) + n(t), \quad 0 \leq t \leq T,$$

where the  $\theta_i$  are phase angles. We assume that the phase angles are uniformly distributed and that each frequency is equally likely to occur. A comparison of the likelihood ratios<sup>1</sup> yields the receiver depicted in figure 2. The decision rule is the following: choose  $H_i$ ,  $i = 1, \dots, M$ , if the largest envelope detector output is greater than the threshold, and choose  $H_0$  otherwise. If a signal is detected, this receiver automatically identifies the frequency as the center frequency of the filter with the largest output.

The matched filters of figure 2 are matched to intercepted signals that are pulsed sinusoids. To accommodate more general, unknown signals, the matched filters could be replaced by bandpass filters. However, such a replacement would give a detector that is not necessarily optimum.

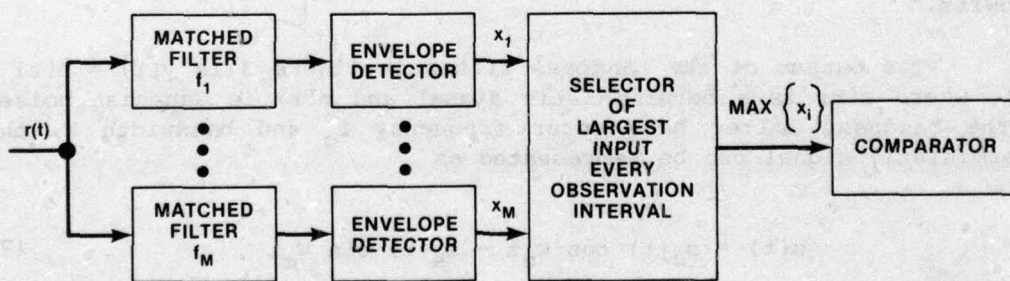


Figure 2. Optimum detector for pulsed sinusoid of unknown frequency.

<sup>1</sup>A. Whalen, *Detection of Signals in Noise*, Academic Press, Inc., New York (1971).

There remain other problems with this receiver. It is doubtful that the envelope detectors can function efficiently against some signal forms. Furthermore, the receiver is designed to operate on a single pulse. Multiple-pulse operation, which may be necessary for detection at low signal power levels, requires additional hardware.

## 2.1 Radiometer

Another approach is to model the signal as a stationary Gaussian process with a flat power spectral density. Assuming that the noise present is white and Gaussian, detection theory yields the optimum receiver depicted in figure 3, which is called an energy detector or a radiometer.<sup>2</sup> This receiver has the major advantages that it requires relatively little hardware and no additional hardware is needed for multiple-pulse detection. The detection of spread spectrum communications presents no special problem.

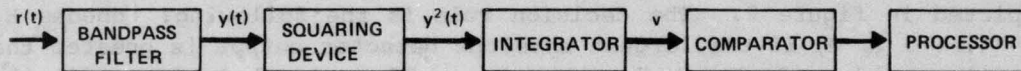


Figure 3. Radiometer.

Although the radiometer is optimum if we model the signal as a stationary Gaussian process, it is intuitively clear that this receiver is a reasonable configuration for determining the presence of unknown deterministic signals. We now give a performance analysis of the detector, assuming a deterministic signal. The original analysis was done by Urkowitz.<sup>3</sup>

The output of the bandpass filter in figure 3 is  $y(t) = s(t) + n(t)$ , where  $s(t)$  is a deterministic signal and  $n(t)$  is Gaussian noise. If the bandpass filter has center frequency  $f_c$  and bandwidth  $W$ , the deterministic signal can be represented as

$$s(t) = s_c(t) \cos \omega_c t - s_s(t) \sin \omega_c t, \quad (7)$$

where  $\omega_c = 2\pi f_c$ . Since the spectrum of  $s(t)$  is confined within the filter bandwidth,  $s_c(t)$  and  $s_s(t)$  have frequency components confined to

<sup>2</sup>H. L. Van Trees, *Detection, Estimation, and Modulation Theory, III*, John Wiley and Sons, Inc., New York (1971).

<sup>3</sup>H. Urkowitz, *Energy Detection of Unknown Deterministic Signals*, *Proc. IEEE*, 55 (April 1967), 523.

the band  $|f| < W/2$ . The Gaussian noise emerging from the bandpass filter can be represented in terms of quadrature components as<sup>4</sup>

$$n(t) = n_c(t) \cos \omega_c t - n_s(t) \sin \omega_c t . \quad (8)$$

If  $n(t)$  is filtered white noise of spectral density  $N_0/2$ , then  $n_c(t)$  and  $n_s(t)$  have flat power spectral densities, each equal to  $N_0$  over  $|f| < W/2$ .

As shown in figure 3, the input to the comparator is

$$V(t) = \int_{t-T}^t y^2(\tau) d\tau , \quad (9)$$

where the integration interval is equal to the observation interval,  $T$ .

The comparator output may be sampled or continuously fed to a processor. We next determine the probabilities of false alarm and detection associated with  $V(t)$  at a fixed time. For convenience, we normalize the test statistic to

$$v = \frac{2}{N_0} \int_0^T y^2(t) dt . \quad (10)$$

Substituting equations (7) and (8) and assuming that  $f_c T \gg 1$ ,  $f_c \gg W$ , we obtain the approximation

$$v = \frac{1}{N_0} \int_0^T [s_c(t) + n_c(t)]^2 dt + \frac{1}{N_0} \int_0^T [s_s(t) + n_s(t)]^2 dt . \quad (11)$$

From the sampling theorems for deterministic and stochastic processes,<sup>5</sup> respectively, we obtain expressions that facilitate a statistical performance analysis. After an appropriate choice of time origin, we may write

<sup>4</sup>R. E. Ziemer and W. H. Tranter, *Systems, Modulation and Noise*, Houghton Mifflin Co., New York (1976).

<sup>5</sup>A. Papoulis, *Signal Analysis*, McGraw-Hill Book Co., New York (1977).

$$s_c(t) = \sum_{i=-\infty}^{\infty} s_c\left(\frac{i}{W}\right) \text{sinc}(Wt - i), \quad (12)$$

$$s_s(t) = \sum_{i=-\infty}^{\infty} s_s\left(\frac{i}{W}\right) \text{sinc}(Wt - i), \quad (13)$$

$$n_c(t) = \sum_{i=-\infty}^{\infty} n_c\left(\frac{i}{W}\right) \text{sinc}(Wt - i), \quad (14)$$

$$n_s(t) = \sum_{i=-\infty}^{\infty} n_s\left(\frac{i}{W}\right) \text{sinc}(Wt - i), \quad (15)$$

where  $\text{sinc } x = \sin \pi x / \pi x$ . We make the following approximations, based upon the known properties of the sinc function:

$$\int_0^T \text{sinc}(Wt - i) \text{sinc}(Wt - j) dt \approx 0, \quad i \neq j, \quad (16)$$

$$\int_0^T \text{sinc}^2(Wt - i) dt \approx \int_{-\infty}^{\infty} \text{sinc}^2(Wt - i) dt = \frac{1}{W}, \quad 0 < i \leq TW, \quad (17)$$

$$\int_0^T \text{sinc}^2(Wt - i) dt \approx 0, \quad i \leq 0 \text{ or } i > TW. \quad (18)$$

The error introduced by each integral approximation is bounded by  $1/2W$ . Assuming that  $TW \geq 1$ , the error introduced by equation (18) at  $i = 0$  is nearly  $1/2W$ . For other values of  $i$ , except possibly  $i = TW$ , the errors caused by the approximations are much less than  $1/2W$  and decrease as  $TW$  increases. Substituting equations (12) to (18) into equation (11), we obtain

$$v = \frac{1}{N_0 W} \sum_{i=1}^Y \left[ s_c\left(\frac{i}{W}\right) + n_c\left(\frac{i}{W}\right) \right]^2 + \frac{1}{N_0 W} \sum_{i=1}^Y \left[ s_s\left(\frac{i}{W}\right) + n_s\left(\frac{i}{W}\right) \right]^2, \quad (19)$$

where  $\gamma$  is the largest integer less than or equal to  $TW$ . In view of the approximations made, this equation becomes an increasingly accurate approximation of equation (11) as  $\gamma$  increases. It is always assumed that  $\gamma \geq 1$ .

We assume that the bandpass filter has a transfer function that is rectangular about  $f_c$ . Since  $n(t)$  has a power spectral density that is symmetrical about  $f_c$ ,  $n_c(t)$  and  $n_s(t)$  are independent Gaussian processes.<sup>4</sup> Thus,  $n_c(i/W)$  and  $n_s(j/W)$  are independent Gaussian random variables. The power spectral densities of both  $n_c(t)$  and  $n_s(t)$  are  $S(f) = N_0$  for  $|f| < W/2$  and  $S(f) = 0$  otherwise. The associated autocorrelation function is

$$R(\tau) = N_0 W \text{sinc } W\tau . \quad (20)$$

This expression indicates that  $n_c(i/W)$  is statistically independent of  $n_c(j/W)$ ,  $i \neq j$ , and similarly for  $n_s(i/W)$  and  $n_s(j/W)$ . If  $n(t)$  is assumed to be zero-mean, so are  $n_c(i/W)$  and  $n_s(i/W)$ . Using these facts, we rewrite equation (19) as

$$v = \sum_{i=1}^{\gamma} a_i^2 + \sum_{i=1}^{\gamma} b_i^2 , \quad (21)$$

where the  $a_i$ 's and the  $b_i$ 's are statistically independent Gaussian random variables with unit variances and means

$$m_{1i} = E[a_i] = \frac{1}{(N_0 W)^{1/2}} s_c \left( \frac{i}{W} \right) , \quad (22)$$

$$m_{2i} = E[b_i] = \frac{1}{(N_0 W)^{1/2}} s_s \left( \frac{i}{W} \right) . \quad (23)$$

The first sum in equation (21) has a noncentral  $\chi^2$  distribution<sup>1</sup> with  $\gamma$  degrees of freedom and a noncentral parameter  $\lambda_1 = \sum m_{1i}^2$ . Similarly, the second sum has a noncentral  $\chi^2$  distribution with  $\gamma$  degrees of freedom and a noncentral parameter  $\lambda_2 = \sum m_{2i}^2$ . Since the two

<sup>1</sup>A. Whalen, *Detection of Signals in Noise*, Academic Press, Inc., New York (1971).

<sup>4</sup>R. E. Ziemer and W. H. Tranter, *Systems, Modulation and Noise*, Houghton Mifflin Co., New York (1976).

$\chi^2$  variables are independent,  $V$  has a noncentral  $\chi^2$  distribution with  $2Y$  degrees of freedom and noncentral parameter  $\lambda = \lambda_1 + \lambda_2$ . Thus,

$$\begin{aligned} \lambda &= \frac{1}{N_0 W} \sum_{i=1}^Y s_c^2\left(\frac{i}{W}\right) + \frac{1}{N_0 W} \sum_{i=1}^Y s_s^2\left(\frac{i}{W}\right) \\ &\approx \frac{1}{N_0} \int_0^T [s_c^2(t) + s_s^2(t)] dt \\ &\approx \frac{2}{N_0} \int_0^T s^2(t) dt . \end{aligned} \quad (24)$$

In terms of the signal energy,  $E$ , we have the approximation

$$\lambda = \frac{2E}{N_0} . \quad (25)$$

By straightforward calculations using the statistics of Gaussian variates, the mean and the variance of  $V$  are determined to be

$$E[V] = \lambda + 2Y , \quad (26)$$

$$\text{VAR}(V) = 4\lambda + 4Y . \quad (27)$$

By using the known probability density functions for a noncentral  $\chi^2$  random variable, the false alarm and detection probabilities can be expressed as integrals. In the absence of a signal, the  $\chi^2$  probability density function for  $V$  is

$$p_0(v) = \frac{1}{2^Y \Gamma(Y)} v^{Y-1} e^{-v/2} , \quad v \geq 0 \quad (28)$$

$$p_0(v) = 0 , \quad v < 0$$

where  $\Gamma(x)$  is the gamma function. The false alarm probability is

$$P_F = \int_{V_T}^{\infty} p_0(v) dv . \quad (29)$$

If the signal is present, the  $\chi^2$  probability density function for  $V$  is

$$p_1(v) = \frac{1}{2} \left( \frac{v}{\lambda} \right)^{(\gamma-1)/2} \exp \left( -\frac{v+\lambda}{2} \right) I_{\gamma-1}(\sqrt{v\lambda}), \quad v \geq 0,$$

$$p_1(v) = 0, \quad v < 0, \quad (30)$$

where  $I_n(x)$  is the modified Bessel function of the first kind and order  $n$ . The probability of detection is

$$P_D = \int_{V_T}^{\infty} p_1(v) dv. \quad (31)$$

Numerous schemes for evaluating  $P_F$  and  $P_D$  have been proposed in the literature.<sup>1,3</sup>

We are particularly interested in the case in which  $TW$  is large since this case includes the interception of spread spectrum communications. When  $TW$  is large,  $\gamma \approx TW$ , and the central limit theorem indicates that  $V$  is approximated by a Gaussian variate. Using equations (26) and (27) with  $\lambda = 0$  and equation (29) with a Gaussian density for  $p_0(v)$ , we obtain

$$P_F = \frac{1}{(8\pi TW)^{1/2}} \int_{V_T}^{\infty} \exp \left[ -\frac{(v - 2TW)^2}{8TW} \right] dv$$

$$= \frac{1}{2} \operatorname{erfc} \left[ \frac{V_T - 2TW}{(8TW)^{1/2}} \right]. \quad (32)$$

Similarly, we obtain

$$P_D = \frac{1}{2} \operatorname{erfc} \left[ \frac{V_T - 2TW - \lambda}{(8TW + 8\lambda)^{1/2}} \right]. \quad (33)$$

<sup>1</sup>A. Whalen, *Detection of Signals in Noise*, Academic Press, Inc., New York (1971).

<sup>3</sup>H. Urkowitz, *Energy Detection of Unknown Deterministic Signals*, *Proc. IEEE*, 55 (April 1967), 523.

Combining equations (4), (5), (32), and (33) gives

$$(8TW + 8\lambda)^{1/2} \xi = (8TW)^{1/2} \beta - \lambda . \quad (34)$$

We can solve this equation to determine the value of  $E/N_0$  necessary to achieve specified values of  $P_F$  and  $P_D$ . Solving for  $\lambda$  and using equation (25), we obtain

$$\frac{E}{N_0} = 2\xi^2 + \beta(2TW)^{1/2} - \xi \left[ 2TW + 4\xi^2 + 2\beta(8TW)^{1/2} \right]^{1/2} . \quad (35)$$

If we assume that  $TW \gg \beta^2$  and  $TW \gg \xi^2$ , then further simplification is possible. The result is

$$\frac{E}{N_0} = (2TW)^{1/2} (\beta - \xi) , \quad TW \gg \max(\beta^2, \xi^2) . \quad (36)$$

Comparing equations (36) and (6), we see that the disparity in performance between the radiometer and the matched filter increases with  $TW$ . Equation (36) indicates that detection difficulties increase as the intercepted signal spectrum is spread.

Denoting the intercepted signal power by  $R_S$  and the signal duration by  $T_1$ , the intercepted power necessary to achieve specified values of  $P_F$  and  $P_D$  is

$$R_S = N_0 \frac{(2TW)^{1/2}}{T_1} (\beta - \xi) , \quad T_1 < T , \quad TW \gg \max(\beta^2, \xi^2) ,$$

$$R_S = N_0 \left( \frac{2W}{T} \right)^{1/2} (\beta - \xi) , \quad T_1 \geq T , \quad TW \gg \max(\beta^2, \xi^2) . \quad (37)$$

As long as  $T_1 \geq T$ , this equation indicates that increasing the observation interval decreases the required power. However, if  $T_1 < T$ , an increase in the observation interval increases the required power.

If the outputs of  $N_r$  independent radiometers are averaged, a straightforward calculation shows that the required  $R_S$  can be reduced by a factor of  $N_r^{-1/2}$ .



## 2.2 Channelized Radiometer

A channelized radiometer forms when  $M$  radiometers are inserted in the branches of figure 2, as depicted in figure 4(a). Each block labeled radiometer contains a bandpass filter of bandwidth  $W/M$ , a squaring device, and an integrator, but no comparator. Let  $T_s$  denote the sampling interval, which is the observation interval of the constituent radiometers. To avoid processing extraneous noise, the arrival time of the signal to be intercepted may be estimated by additional hardware. The sampling interval may equal or be somewhat less than the minimum expected signal duration in a channel. To increase effectiveness against frequency hopping or multiple frequency-shift keying (MFSK), the processor examines  $N$  consecutive comparator outputs and determines that a signal is present if  $r$  of these outputs correspond to comparator inputs that exceed the threshold. For example, if  $N$  is odd, a majority decision rule requires  $r = (N + 1)/2$ . The effective observation interval of the channelized radiometer, given by  $T = NT_s$ , should usually be less than the minimum expected message duration. If it is known that the intercepted signal is narrowband, we can set  $N = 1$ . If the presence of more than one signal is to be verified, it is desirable to employ an array of radiometers of the form of figure 3 with the comparator outputs feeding into a processor that analyzes the activity of individual channels, as shown in figure 4(b). In this configuration,  $N = 1$  and each bandpass filter has a bandwidth of  $W/M$ .

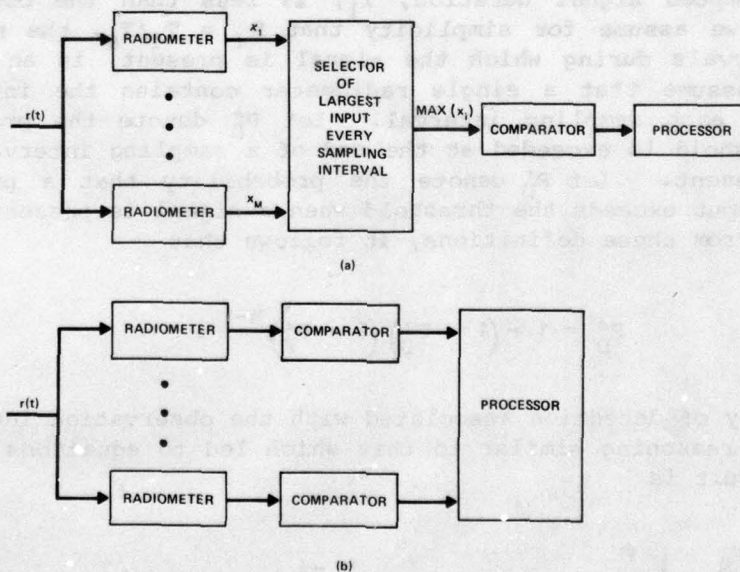


Figure 4. Channelized radiometers (a) for detection of presence of hostile communications and (b) for simultaneous detection of multiple signals.

To simplify the analysis of the interception of a single signal, we assume that the  $N$  sets of radiometer outputs are statistically independent. If  $P'_F$  is the probability that a particular radiometer output exceeds the threshold when no signal is present, then the probability that none of the radiometer outputs exceeds the threshold is  $(1 - P'_F)^M$ , assuming that the channel noises are statistically independent. The probability that exactly  $i$  out of  $N$  comparator inputs exceeds the threshold is

$$P(i, N) = \binom{N}{i} \left[ 1 - (1 - P'_F)^M \right]^i (1 - P'_F)^{M(N-i)}, \quad i \leq N,$$

$$P(i, N) = 0, \quad i > N. \quad (38)$$

It follows that the probability of false alarm associated with the observation interval is

$$P_F = \sum_{i=r}^N P(i, N). \quad (39)$$

If the intercepted signal duration,  $T_1$ , is less than the observation interval,  $T$ , we assume for simplicity that  $N_1 = T_1/T_s$ , the number of sampling intervals during which the signal is present, is an integer. Further, we assume that a single radiometer contains the intercepted signal during each sampling interval. Let  $P''_D$  denote the probability that the threshold is exceeded at the end of a sampling interval when a signal is present. Let  $P'_D$  denote the probability that a particular radiometer output exceeds the threshold when a signal is present in that radiometer. From these definitions, it follows that

$$P''_D = 1 - (1 - P'_D)(1 - P'_F)^{M-1}. \quad (40)$$

The probability of detection associated with the observation interval is determined by reasoning similar to that which led to equations (38) and (39). The result is

$$P_D = \sum_{i=r}^N \sum_{j=0}^i \binom{N_1}{j} (P''_D)^j (1 - P''_D)^{N_1-j} P(i-j, N - N_1). \quad (41)$$

To compare the channelized radiometer with a single wideband radiometer, we assume that  $N = N_1$  and that the energy of the intercepted signal is equally divided among the  $N$  sampling intervals. Since the total receiver bandwidth is  $W$ , the bandwidth of each constituent radiometer is  $W_s = W/M$ . Thus, for large values of  $T_s W_s$ ,  $P'_F$  and  $P'_D$  are given by equations (32) and (33) with  $W_s = W/M$  substituted for  $W$ ,  $T_s = T/N$  substituted for  $T$ , and  $\lambda_s = \lambda/N$  substituted for  $\lambda$ . We have

$$P'_F = \frac{1}{2} \operatorname{erfc} \left[ \frac{MN V_T - 2TW}{(8TWMN)^{1/2}} \right], \quad (42)$$

$$P'_D = \frac{1}{2} \operatorname{erfc} \left[ \frac{MN V_T - 2TW - \lambda M}{(8TWMN + 8\lambda M^2 N)^{1/2}} \right]. \quad (43)$$

We define

$$\beta_1 = \operatorname{erfc}^{-1} (2P'_F), \quad (44)$$

$$\xi_1 = \operatorname{erfc}^{-1} (2P'_D). \quad (45)$$

If  $P'_F$  and  $P'_D$  are specified, we solve equations (38) to (41) for  $P'_F$  and  $P'_D$ . Using equations (42) to (45), we perform a calculation analogous to that used in deriving equation (37). The result is that the required  $R_s$  for detection with specified values of  $P'_F$  and  $P'_D$  is

$$R_s \approx N_0 \left( \frac{2WN}{MT} \right)^{1/2} (\beta_1 - \xi_1), \quad T_1 \geq T, \quad TW \gg MN \max(\beta_1^2, \xi_1^2). \quad (46)$$

If a frequency-hopping signal is to be intercepted, the parameter  $N$  is proportional to the hopping rate. Thus, equation (46) indicates that the required power is proportional to the square root of the hopping rate. If  $M \gg N$ , the channelized radiometer requires less power than a wideband radiometer with the same values of  $T$  and  $W$ . If we set  $N = 1$  and attempt to intercept a frequency-hopping signal by processing each hop, then  $T$  must be decreased as the hopping rate increases.

Suppose that the energy is concentrated in a narrow bandwidth during the observation interval and that the bandwidths of the radiometers are sufficiently wide so that the energy enters a single radiometer. Then we may take  $r = N = N_1 = 1$ . Equations (39) and (41) reduce to

$$P_F = 1 - (1 - P'_F)^M, \quad (47)$$

$$P_D = 1 - (1 - P'_D)(1 - P'_F)^{M-1}. \quad (48)$$

The required value of  $R_S$  for detection is determined by the usual method to be

$$R_S \approx N_0 \left( \frac{2W}{MT} \right)^{1/2} (\beta_1 - \xi_1), \quad T_1 \geq T, \quad TW \gg M \max(\beta_1^2, \xi_1^2), \quad (49)$$

where

$$\beta_1 = \operatorname{erfc}^{-1} \left[ 2 - 2(1 - P_F)^{1/M} \right], \quad (50)$$

$$\xi_1 = \operatorname{erfc}^{-1} \left[ 2 - \frac{2(1 - P_D)}{(1 - P_F)^{1-1/M}} \right]. \quad (51)$$

Thus, the required power falls approximately as the square root of the number of channels.

To determine  $P'_F$  and  $P'_D$  when equations (42) and (43) do not apply, we assume that the intercepted signal energy is equally divided among the  $N_1$  sampling intervals. We use equations (28) to (31) with  $\lambda_s = \lambda/N_1$  substituted for  $\lambda$  and  $\eta$ , the largest integer less than or equal to  $T_S \bar{W}_S$ , substituted for  $\gamma$ . The results are

$$P'_F = \frac{1}{2^n \Gamma(\eta)} \int_{V_T}^{\infty} v^{\eta-1} \exp\left(-\frac{v}{2}\right) dv, \quad (52)$$

$$P'_D = \frac{1}{2} \int_{V_T}^{\infty} \left( \frac{v}{\lambda_s} \right)^{(\eta - 1)/2} \exp \left( - \frac{v + \lambda_s}{2} \right) I_{\eta-1} \left( \sqrt{v \lambda_s} \right) dv \quad (53)$$

By numerical methods, this pair of equations can be solved simultaneously to eliminate  $V_T$  and express  $\lambda = N_1 \lambda_s$  as a function of  $P'_F$  and  $P'_D$ . If we solve equations (38) to (41) for  $P'_F$  and  $P'_D$  in terms of  $P_F$  and  $P_D$ , then we can obtain an equation for  $\lambda$  in terms of  $P_F$  and  $P_D$ . From this equation, we finally obtain the required value of  $R_S$  necessary to achieve specified values of  $P_F$  and  $P_D$ .

The channelized radiometer has been shown to be relatively effective against conventional and frequency-hopping communications. It is also useful against pseudonoise spread spectrum communications if preliminary processing is used to produce a signal with a narrow bandwidth (sect. 3).

### 2.3 Cross Correlator

The ideal correlator of figure 1 can be approximated if the signal is intercepted at two spatially separated antennas. The cross-correlation function of the two antenna outputs is estimated for various relative arrival times, and the peak value of this function is applied to a comparator. Figure 5 is a block diagram of a realization employing the discrete Fourier transform (DFT). One way to implement the DFT is to use a digital filter and the fast Fourier transform algorithm. An alternative implementation is to use the chirp Z-transform algorithm and charge-coupled devices. An analog realization of the cross-correlation function that is similar to the configuration of figure 5 can be accomplished with dispersive filters providing Fourier transforms (sect. 3.6). Elegant realizations are possible with acousto-optical devices.<sup>6</sup>

Figure 5a depicts the initial processing of each antenna output. After passage through the bandpass filter of bandwidth  $W$ , the intercepted waveform,  $r(t) = s(t) + n(t)$ , can be represented as

$$r(t) = r_c(t) \cos \omega_c t - r_s(t) \sin \omega_c t \quad (54)$$

where the quadrature components,  $r_c(t)$  and  $r_s(t)$ , are confined to the band  $|f| \leq W/2$ . If the two lowpass filters have bandwidths  $W/2$  and  $f_c = \omega_c/2\pi > W/2$ , then  $r_c(t)$  and  $r_s(t)$  are extracted by the operations shown in figure 5(a). Analog-to-digital converters produce the discrete sequences  $r_c(i/W)$  and  $r_s(i/W)$ .

<sup>6</sup>R. A. Sprague, *A Review of Acousto-optic Signal Correlators*, *Optical Engineering*, 16 (September 1977), 467.

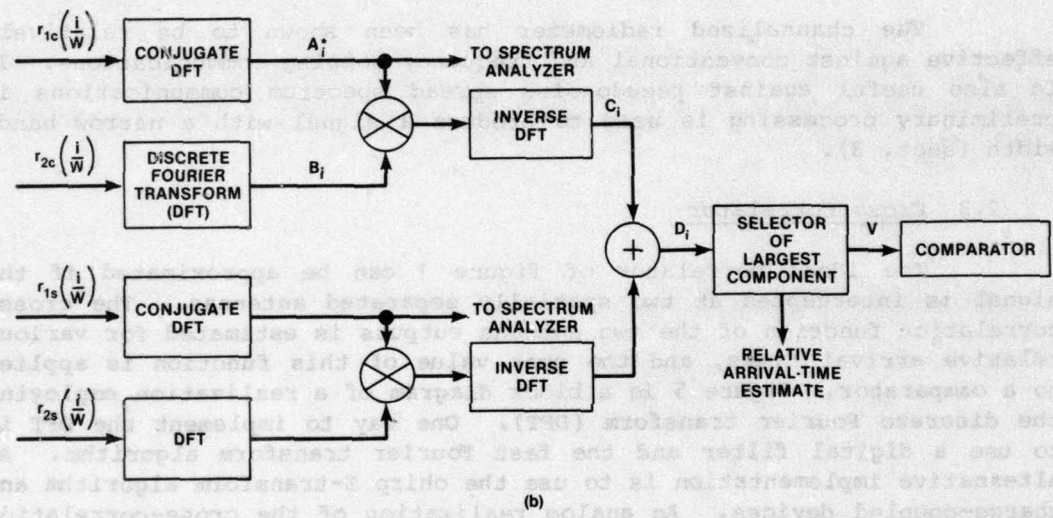
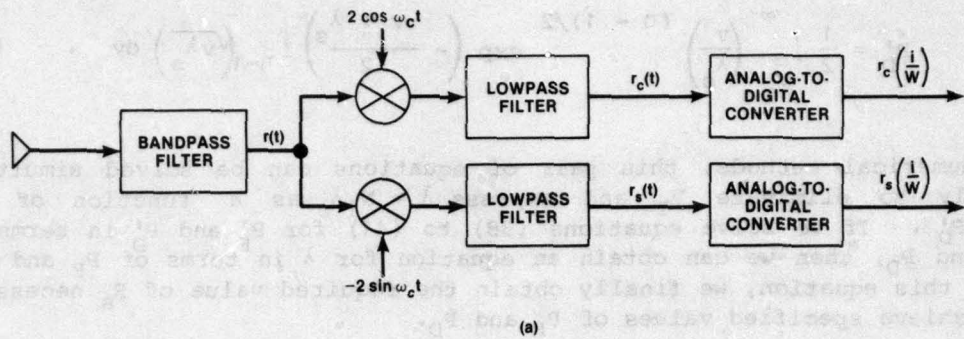


Figure 5. Cross correlator: (a) initial processing of each antenna output and (b) final processing.

We regard one of the antennas as a reference and denote its output by the subscript 1. In terms of the signal and the noise, we have

$$r_1(t) = s(t) + n_1(t) \quad , \quad (55)$$

$$r_{1c}(t) = s_c(t) + n_{1c}(t) \quad , \quad (56)$$

$$r_{1s}(t) = s_s(t) + n_{1s}(t) \quad . \quad (57)$$

Denoting the output of the other antenna by the subscript 2, we have

$$r_2(t) = s(t - T_r) + n_2'(t) , \quad (58)$$

$$r_{2c}(t) = s_c(t - T_r) + n_{2c}'(t) , \quad (59)$$

$$r_{2s}(t) = s_s(t - T_r) + n_{2s}'(t) , \quad (60)$$

where  $T_r$  is the arrival time of the intercepted signal at this antenna output relative to the arrival time at the reference antenna output. By inserting a sufficiently long delay before this antenna output, we ensure that  $T_r \geq 0$ . It is convenient to use the notation

$$a_i = r_{1c} \left( \frac{i+1}{W} \right) , \quad i = 0, 1, \dots, \gamma - 1, \quad (61)$$

$$b_i = r_{2c} \left( \frac{i+1}{W} \right) , \quad i = 0, 1, \dots, \gamma - 1$$

for two of the discrete sequences observed during the interval  $T$ . We form sequences with  $K = \gamma + N_c - 1$  points by augmenting the  $a_i$  and  $b_i$  with  $N_c - 1$  zeros, where  $N_c \leq \gamma$ . As indicated in figure 5(b), the conjugate DFT of  $a_i$  is calculated, giving

$$A_i^* = \sum_{n=0}^{K-1} a_n \Omega_K^{-in} , \quad i = 0, 1, \dots, K - 1, \quad (62)$$

where  $\Omega_K = \exp(-j2\pi/K)$  and  $j = \sqrt{-1}$ . Similarly, the DFT of  $b_i$  is

$$B_i = \sum_{n=0}^{K-1} b_n \Omega_K^{in} , \quad i = 0, 1, \dots, K - 1 . \quad (63)$$

The inverse DFT of the product  $A_i^* B_i$  for  $0 \leq N_c - 1$  is

$$\begin{aligned}
 C_i &= \frac{1}{K} \sum_{n=0}^{K-1} A_n^* B_n \Omega_K^{-in} \\
 &= \frac{1}{K} \sum_{m=0}^{K-1} \sum_{k=0}^{K-1} a_m b_k \sum_{n=0}^{K-1} \Omega_K^{n(-m+k-i)} \\
 &= \sum_{k=0}^{\gamma-1} \sum_{m=0}^{\gamma-1} a_m b_k \delta_{m,k-i} = \sum_{k=i}^{\gamma-1} a_{k-i} b_k, \quad (64)
 \end{aligned}$$

where  $\delta_{ik}$  is the Kronecker delta. From the original definitions and equations similar to equations (12) to (18), we obtain for  $i \ll TW$ ,

$$\begin{aligned}
 C_i &= \sum_{k=i}^{\gamma-1} r_{1c} \left( \frac{k+1-i}{W} \right) r_{2c} \left( \frac{k+1}{W} \right) \\
 &\approx W \int_{i/W}^T r_{1c} \left( t - \frac{i}{W} \right) r_{2c}(t) dt. \quad (65)
 \end{aligned}$$

This sequence is the output of one of the inverse DFT operations shown in figure 5(b). An analogous expression can be written for the output of the other inverse DFT operation. The addition of the two sequences produces a sequence proportional to

$$D_i = \int_{i/W}^T \left[ r_{1c} \left( t - \frac{i}{W} \right) r_{2c}(t) + r_{1s} \left( t - \frac{i}{W} \right) r_{2s}(t) \right] dt. \quad (66)$$

If  $f_c \gg W$ , then expansions similar to equation (54) lead to the approximation

$$D_i = \int_{i/W}^T 2r_1 \left( t - \frac{i}{W} \right) r_2(t) dt, \quad i = 0, 1, \dots, N_c - 1. \quad (67)$$



To interpret the next operation in figure 5(b), we initially assume that no noise is present. In this case, equations (55) and (58) yield

$$D_i = \int_{i/W}^T 2s(t - \frac{i}{W}) r_r(t - T_r) dt, \quad i = 0, 1, \dots, N_c - 1. \quad (68)$$

Thus, the  $D_i$  provide sampled values of an approximation of the autocorrelation function of  $s(t)$ . Let  $i_0$  denote the index that corresponds to the largest  $D_i$ . Assuming that the approximation is adequate and that the autocorrelation function has a sharp peak,  $i_0$  is the index closest to the value  $T_r W$ . When noise is present, this statement may not be true; however, to proceed with the analysis, we assume that it is. Note that  $T_r$  can be estimated as  $i_0/W$ . This estimate can be used for direction finding (sect. 4.2).

Assuming that the largest  $D_i$  has index  $i_0 = T_r W \leq N_c - 1$  and normalizing, the input to the comparator in figure 5(b) is the test statistic

$$\begin{aligned} V &= \frac{2}{N_0 T_r} \int_0^T r_1(t - T_r) r_2(t) dt \\ &= \frac{2}{N_0} \int_0^{T-T_r} r_1(t) r_2(t + T_r) dt. \end{aligned} \quad (69)$$

Substituting equations (55) and (58) and defining  $n_2(t) = n_1'(t + T_r)$  and  $T_a = T - T_r$ , we get

$$V = \frac{2}{N_0} \int_0^{T_a} [s(t) + n_1(t)] [s(t) + n_2(t)] dt. \quad (70)$$

In the usual manner, we obtain the series expansion

$$\begin{aligned} V &= \frac{1}{N_0 W} \sum_{i=1}^{Y_a} \left[ s_c\left(\frac{i}{W}\right) + n_{1c}\left(\frac{i}{W}\right) \right] \left[ s_c\left(\frac{i}{W}\right) + n_{2c}\left(\frac{i}{W}\right) \right] \\ &+ \frac{1}{N_0 W} \sum_{i=1}^{Y_a} \left[ s_s\left(\frac{i}{W}\right) + n_{1s}\left(\frac{i}{W}\right) \right] \left[ s_s\left(\frac{i}{W}\right) + n_{2s}\left(\frac{i}{W}\right) \right], \end{aligned} \quad (71)$$

where  $\gamma_a$  is the largest integer less than or equal to  $T_a W$ . Assuming that  $n_1(t)$  and  $n_2(t)$  are statistically independent, zero-mean, Gaussian processes, a straightforward calculation yields

$$E[V] = \lambda_a \quad (72)$$

$$\text{VAR}(V) = 2\lambda_a + 2\gamma_a \quad (73)$$

where  $\lambda_a = 2E_a/N_0$  and  $E_a$  is the energy in interval  $T_a$ .

For large values of  $T_a W$ , the test statistic is approximately normally distributed. It follows that

$$P_D = \frac{1}{2} \operatorname{erfc} \left[ \frac{V_T - \lambda_a}{(4T_a W + 4\lambda_a)^{1/2}} \right] \quad (74)$$

According to equation (67), the cross-correlation function is computed for  $N_C$  sample values. However, the maximum possible value of  $T_r$  may be such that only  $N_C \ll \gamma$  sample values need to be computed to obtain  $V$ . When no signal is present, a false alarm occurs if any of the  $N_C$  estimated cross-correlation values exceeds the threshold. If  $N_C$  is sufficiently small, it is reasonable to assume that each estimated value has approximately the same probability, denoted by  $P'_F$ , of exceeding the threshold. This assumption implies the approximation,

$$P_F = 1 - (1 - P'_F)^{N_C} \quad (75)$$

where  $P'_F$  is the probability that

$$v = \int_0^{T_a} n_1(t) n_2(t) dt \quad (76)$$

exceeds the threshold. The mean and the variance of equation (76) are given by equations (72) and (73) with  $\lambda_a = 0$ . For large values of  $T_a W$ , we obtain

$$P'_F = \operatorname{erfc} \left[ \frac{V_T}{(4T_a W)^{1/2}} \right] \quad (77)$$

Equations (44) and (75) yield

$$\beta_1 = \operatorname{erfc}^{-1} \left[ 2 - 2(1 - P_F)^{1/N_C} \right] \quad (78)$$

We obtain in the usual manner the required  $R_S$  to detect a signal with specified values of  $P_F$  and  $P_D$ . The result is

$$R_S \approx N_0 \frac{(T_a W)^{1/2}}{T_1} (\beta_1 - \xi), \quad T_1 < T_a, \quad T_a W \gg \max(\beta_1^2, \xi^2), \quad (79)$$

$$R_S \approx N_0 \left(\frac{W}{T_a}\right)^{1/2} (\beta_1 - \xi), \quad T_1 \geq T_a, \quad T_a W \gg \max(\beta_1^2, \xi^2),$$

where  $T_1$  is the signal duration.

Comparison with equation (37) indicates that the cross correlator can give a theoretical improvement of approximately 1.5 dB over a single wideband radiometer. Taking into account the approximations made to derive equation (79), it is possible that in practice the cross correlator provides no improvement at all. A comparison of figures 3 and 5 indicates that the implementation of the cross correlator entails considerably more hardware than the implementation of a wideband radiometer. However, as discussed in subsequent sections, the cross correlator requires little additional hardware to provide frequency estimation and direction finding.

The channelized cross correlator is an array of  $M$  cross correlators, each of which has a bandwidth of  $W/M$ . The outputs of the array are applied to a processor. Analogously to the channelized radiometer, the channelized cross correlator may be preferable to a single wideband cross correlator when the hostile communications are narrowband or when two or more simultaneous signals are to be intercepted.

Equations (37) and (79) indicate that increasing the bandwidth of a frequency-hopping system degrades the performance against a single signal of both the wideband cross correlator and the wideband radiometer. However, neither of these receivers is sensitive to the hopping

rate. Increasing the hopping rate makes the practical design of a channelized receiver more difficult and degrades its performance. If the rate is sufficiently high, the channelized receiver may have to be abandoned in favor of a wideband receiver.

### 3. FREQUENCY ESTIMATION

The immediate purpose of a frequency estimation system is to determine the center frequency and possibly the spectral shape of an intercepted signal. If a frequency-hopping signal is intercepted, the purpose is to determine each hopping frequency or at least the frequency range over which the hopping occurs.

Although not desirable for some purposes, such as message analysis, preliminary processing of pseudonoise spread-spectrum communications is desirable before estimation of the center frequency is attempted. An intercepted binary pseudonoise signal has the form

$$s(t) = Am(t)p(t) \cos \omega_0 t, \quad (80)$$

where  $A$  is the amplitude,  $\omega_0$  is the center frequency,  $m(t)$  is the binary message sequence, and  $p(t)$  is a binary pseudorandom sequence. Both  $m(t)$  and  $p(t)$  take the values  $+1$  or  $-1$ . Suppose  $s(t)$  enters a wideband receiver and is squared. Since  $m^2 = p^2 = 1$ , the output of the squaring device is proportional to

$$s^2(t) = A^2 \cos^2 \omega_0 t = \frac{A^2}{2} + \frac{A^2}{2} \cos 2 \omega_0 t. \quad (81)$$

The double-frequency term is now a pure pulsed sinusoid. Its frequency and, thus, the center frequency of  $s(t)$  can be estimated by the systems described in this section. The same preliminary processing is useful against phase-shift keyed communications.

#### 3.1 Channelized Receiver

Estimation theory leads to the receiver of figure 2 for frequency estimation, assuming that the arrival time and the signal waveform, except for a uniformly distributed phase angle, are known.<sup>1</sup> After the largest output is selected, the unknown frequency is estimated as the center frequency of the filter producing the largest output. A practical approximation to this receiver is the channelized radiometer of figure 4.

<sup>1</sup>A. Whalen, *Detection of Signals in Noise*, Academic Press, Inc., New York (1971).

Suppose we desire a frequency resolution of  $\Delta$ , where  $\Delta$  is not less than the Cramer-Rao bound.<sup>1</sup> If the entire range of reconnoitered frequencies is  $W$ , then each filter must have bandwidth  $2\Delta$  and  $M = W/2\Delta$  is the number of required filters to attain the desired accuracy. If the intercepted signal has duration  $T$ , then each filter must have bandwidth  $2/T$  for most of the signal energy to pass through it. Thus, we have

$$\Delta = \frac{1}{T} . \quad (82)$$

If  $M \geq 6$ , the number of required filters can be reduced by arranging the filters in successive stages, as shown in figure 6 for the case in which each stage has the same number of filters. After an intercepted signal passes through the first filter bank, its frequency is theoretically known within an accuracy of  $\Delta_1 = W/2M_s$ , where  $M_s$  is the number of filters in each stage and  $2\Delta_1$  is the bandwidth of the first stage filters. A bank of mixers ensures that the filter outputs are shifted in frequency so that the input to the second stage has a frequency between  $f_{11} - f_{c1} - \Delta_1$  and  $f_{11} - f_{c1} + \Delta_1$ , where  $f_{11}$  is the center frequency of the top filter in the first bank and  $f_{c1}$  is the frequency of a local oscillator. After the input passes through the second filter bank, the frequency is known within an accuracy  $\Delta_2 = \Delta_1/M_s$ , and so on. If  $N_s$  stages of  $M_s$  filters each are employed, then an accuracy of  $\Delta$  is attained if

$$M_s^{N_s} = \frac{W}{2\Delta} \quad (83)$$

The total number of filters required is  $M_s^{N_s}$ . Disadvantages of the channelized receiver of figure 6 relative to that of figure 4 are the increased processing time required for frequency estimation, the reduced amount of noise and interference filtering, and the ambiguities that arise when more than one signal is intercepted.

It is not necessary that each stage have the same number of filters. However, if  $N_s$ ,  $W$ , and  $\Delta$  are fixed, it can easily be shown, using Lagrange multipliers, that the total number of filters is minimized if each stage has approximately the same number of filters (exactly the same number if an integer  $M_s$  exists that satisfies eq [83]). If each stage has the same number of filters and  $W$  and  $\Delta$  are fixed, it can be shown that the total number of filters is minimized if each stage has three filters. (Lagrange multipliers yield  $M_s = e$ , but  $M_s$  must be an integer.)

<sup>1</sup>A. Whalen, *Detection of Signals in Noise*, Academic Press, Inc., New York (1971).

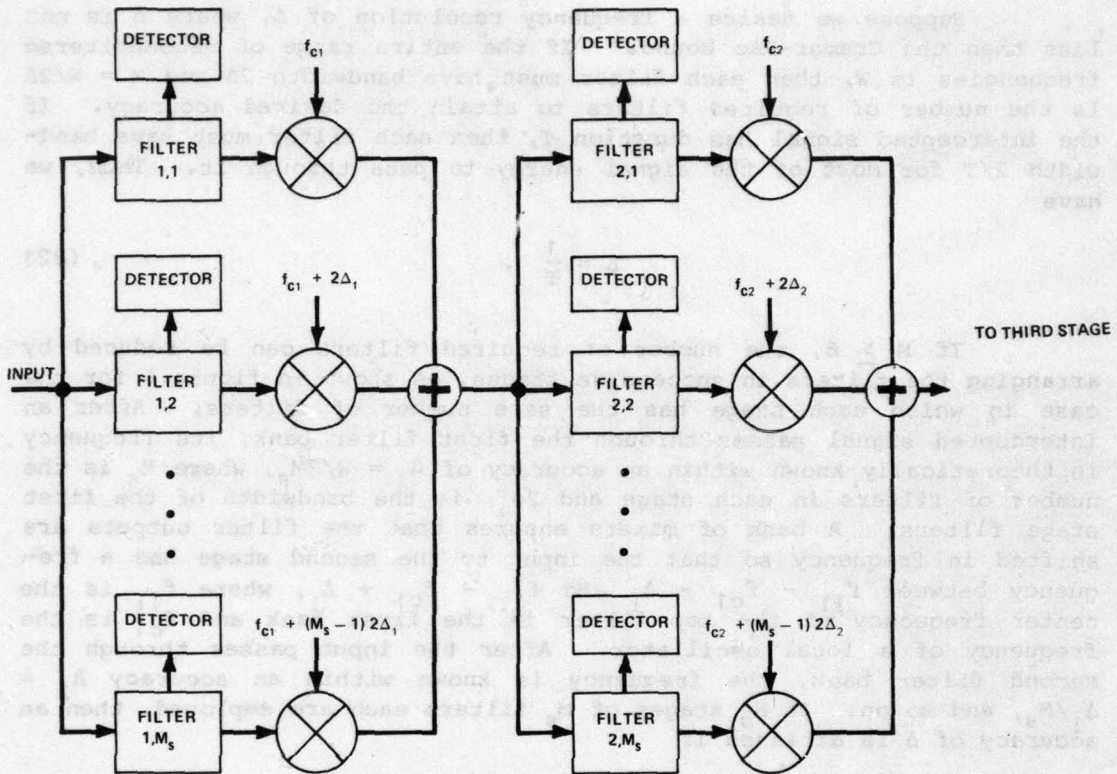


Figure 6. Channelized receiver with filters arranged in successive stages.

Even when minimized, the number of filters and detectors required in a channelized receiver may make this method of frequency estimation expensive. In this case, a limited number of filters can be used to reduce the total bandwidth examined by other frequency estimation devices.

### 3.2 Spectrum Analysis with Discrete Fourier Transform

The outputs of the two conjugate DFT blocks in figure 5(b) provide a scaled phase-shifted estimate of the intercepted spectrum over the receiver bandwidth. To see how the spectrum is estimated, we first define the truncated waveforms:

$$\begin{aligned}
 s'(t) &= s(t)q(t) \quad , \\
 s'_c(t) &= s_c(t)q(t) \quad , \\
 s'_s(t) &= s_s(t)q(t) \quad ,
 \end{aligned}
 \tag{84}$$

where

$$q(t) = 1, \quad 0 < t \leq T,$$

$$q(t) = 0, \quad \text{otherwise} \quad . \quad (85)$$

We denote the Fourier transforms of  $s'(t)$ ,  $s'_c(t)$ , and  $s'_s(t)$  by  $S(\omega)$ ,  $S_c(\omega)$ , and  $S_s(\omega)$ , respectively. From equation (7),

$$S(\omega) = \frac{1}{2} S_c(\omega - \omega_c) + \frac{1}{2} S_c(\omega + \omega_c) - \frac{1}{2j} S_s(\omega - \omega_c) + \frac{1}{2j} S_s(\omega + \omega_c) \quad . \quad (86)$$

We are interested in determining  $S(\omega)$  for  $\omega \geq 0$ . If  $\omega_c \geq \pi W$ , then

$$S(\omega) = \frac{1}{2} S_c(\omega - \omega_c) - \frac{1}{2j} S_s(\omega - \omega_c), \quad \omega \geq 0, \quad \omega_c \geq \pi W \quad . \quad (87)$$

Thus, we can estimate  $S(\omega)$  if we first estimate  $S_c(\omega)$  and  $S_s(\omega)$ .

We give the details of the estimation of  $S_c(\omega)$ ; the estimation of  $S_s(\omega)$  is similar. For simplicity, we assume  $K \approx TW$ . The sample values of  $S_c(\omega)$  are related to those of  $s'_c(t)$  through the fundamental relation<sup>5</sup>

$$\begin{aligned} \bar{S}_c(n\pi) &= \frac{2\pi}{N\pi} \sum_{m=0}^{N-1} \bar{s}_c\left(m \frac{2\pi}{N\pi}\right) \Omega_N^{mn} \\ &= \frac{2\pi}{N\pi} \sum_{m=1}^N \bar{s}_c\left(m \frac{2\pi}{N\pi}\right) \Omega_N^{mn}, \quad n = 0, 1, \dots, N-1, \end{aligned} \quad (88)$$

where  $\Omega_N = \exp(-j2\pi/N)$  and

$$\bar{s}_c(my) = \sum_{k=-\infty}^{\infty} s'_c(my + kNy) \quad , \quad (89)$$

$$\bar{S}_c(n\pi) = \sum_{i=-\infty}^{\infty} S_c(n\pi + iN\pi) \quad . \quad (90)$$

We apply these equations with  $N = \gamma = TW$ ,  $x = 2\pi/T$ , and  $y = 1/W$ . Since  $s'_c(t) = 0$  unless  $0 < t \leq T$ , equation (89) implies that

$$\bar{s}_c\left(\frac{m}{W}\right) = s'_c\left(\frac{m}{W}\right) = s_c\left(\frac{m}{W}\right), \quad 1 \leq m \leq TW. \quad (91)$$

Consequently, equation (88) becomes

$$\bar{S}_c\left(n \frac{2\pi}{T}\right) = \frac{1}{W} \sum_{m=1}^{TW} s_c\left(\frac{m}{W}\right) \Omega_{TW}^{mn}, \quad n = 0, 1, \dots, TW - 1. \quad (92)$$

We assume that  $S(\omega) \approx 0$ , unless  $|\omega - \omega_c| < \pi W$  or  $|\omega + \omega_c| < \pi W$ . Consequently,  $S_c(\omega) \approx 0$  for  $|\omega| \geq \pi W$ , and equation (90) yields the approximate result

$$\bar{S}_c\left(n \frac{2\pi}{T}\right) = S_c\left(n \frac{2\pi}{T}\right), \quad 0 \leq n \leq TW/2,$$

$$\bar{S}_c\left(n \frac{2\pi}{T}\right) = S_c\left(n \frac{2\pi}{T} - 2\pi W\right), \quad TW/2 \leq n \leq TW - 1. \quad (93)$$

Equations (92) and (93) imply that

$$S_c\left(n \frac{2\pi}{T}\right) = \frac{1}{W} \sum_{m=1}^{TW} s_c\left(\frac{m}{W}\right) \Omega_{TW}^{mn}, \quad |n| \leq TW/2. \quad (94)$$

We conclude that, in the presence of noise, a reasonable estimator of the sample values of  $S_c(\omega)$  is given by the right side of equation (94) with  $s_c$  replaced by  $r_{1c}$ . Using equations (61) and (62), we obtain

$$\hat{S}_c\left(n \frac{2\pi}{T}\right) = \frac{1}{W} A_n \Omega_{TW}^n, \quad 0 \leq n \leq TW/2,$$

$$\hat{S}_c\left(n \frac{2\pi}{T}\right) = \frac{1}{W} A_{-n}^* \Omega_{TW}^n, \quad -TW/2 \leq n < 0. \quad (95)$$



If no noise is present, then  $\hat{S}_C(\omega) = S_C(\omega)$  at the sample values. The resolution of  $\hat{S}_C(\omega)$  and  $\hat{S}_S(\omega)$ , the corresponding estimator for  $S_S(\omega)$ , is primarily determined by the duration of the sample pulse.<sup>5</sup> The resolution is

$$\Delta \approx \frac{1}{T} . \quad (96)$$

To obtain a more accurate expression for  $\Delta$ , the effects of the random noise must be evaluated. However, equation (96) is adequate for roughly comparing the frequency estimation potential of the cross correlator with that of competitive systems.

If the frequencies of frequency hopping or MFSK communications are to be successfully estimated, the observation time,  $T$ , must be less than the period between frequency changes.

### 3.3 Acousto-optical Receiver

Spectrum analysis using acousto-optical diffraction has the potential capability for real-time, wideband frequency estimation of many simultaneous signals. The principal components of an acousto-optical spectrum analyzer are shown in figure 7. The diffraction geometry associated with the Bragg cell is illustrated in figure 8. The Bragg cell converts an electronic input at frequency  $f_0$  into a traveling acoustic wave with velocity  $v_a$  and wavelength  $\Lambda_a = v_a/f_0$ . The laser light has wavelength  $\Lambda_o$  in free space and  $\Lambda_o/n$  inside the cell, which has an index of refraction  $n$ . According to Bragg's law, the sound wave interacts with the light beam to produce a principal diffracted beam, which is offset from the incident beam by an angle

$$\theta' = 2 \sin^{-1} \left( \frac{\Lambda_o f_0}{2n v_a} \right) \quad (97)$$

inside the cell and an angle

$$\theta = 2 \sin^{-1} \left( \frac{\Lambda_o f_0}{2v_a} \right) \quad (98)$$

outside the cell. These equations are valid provided that the acoustic wave has a single wavelength across the cell. For small values of the argument, equation (98) becomes

$$\theta \approx \frac{\Lambda_o f_0}{v_a} , \quad \Lambda_o f_0 \ll 2v_a . \quad (99)$$

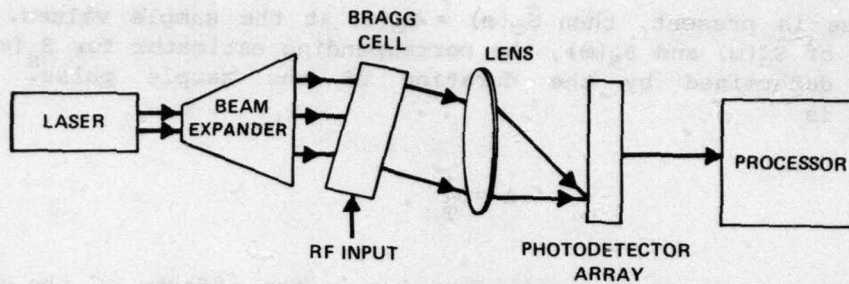


Figure 7. Acousto-optical spectrum analyzer.

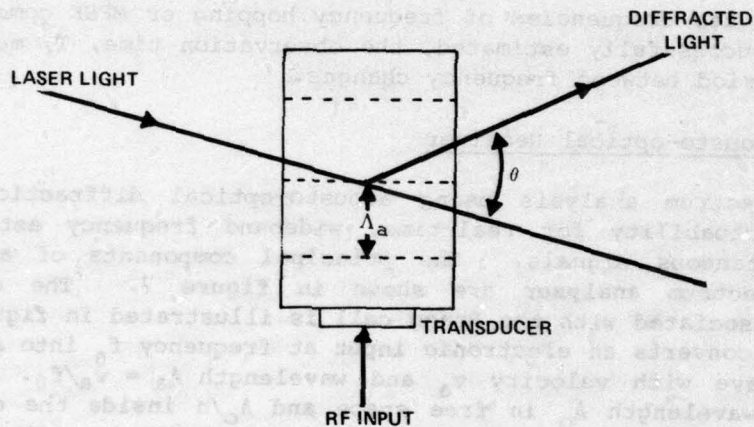


Figure 8. Acousto-optical diffraction geometry for input at single frequency.

The lens produces a Fourier transform on its focal plane at the photodetector array. The center of the diffracted beam converges to a position a distance

$$F\theta = \frac{F\lambda_0 f_0}{v_a} \quad (100)$$

from the center of the corresponding undiffracted beam, where  $F$  is the focal length of the transform lens. Thus, the frequency  $f_0$  can be estimated by measuring the relative intensities at the photodetector array elements.<sup>7</sup>

<sup>7</sup>D. L. Hecht, *Spectrum Analysis Using Acousto-optic Filters*, *Optical Engineering*, 16 (September 1977), 461.

The diffracted beam has an angular width on the order of  $\lambda/D$ , where  $D$  is the effective aperture of the Bragg cell. Consequently, the diffracted beam spreads over length of  $F\lambda/D$  in the focal plane. The frequency resolution is defined to be the difference in frequency between two intercepted signals such that the corresponding positions in the focal plane differ by the spread of the diffracted beam in the focal plane. From this definition and equation (100), the resolution is

$$\Delta \approx \frac{v}{D} a = \frac{1}{T_c} , \quad (101)$$

where  $T_c$  is the time that it takes an acoustic wave to cross the cell aperture. This equation applies when an acoustic wave of fixed wavelength occupies the aperture. A necessary condition for its validity most of the time is that  $T_c$  be less than the period between frequency changes of a frequency-hopping signal or an MFSK signal. Thus, the resolution is no better than the inverse of the hopping period.

In frequency estimation, only one spatial dimension of the Bragg cell is used. It is possible to design a two-dimensional Bragg cell array to estimate frequency and direction of arrival simultaneously,<sup>8</sup> as shown in the schematic diagram of figure 9. The cell inputs are the outputs of spatially separated antennas. The intensity distribution across the photodetector array has one or more maxima that are vertically deflected proportionally to the intercepted signal frequencies and are horizontally deflected proportionally to the signal's angle of arrival. If the largest of the outputs of the photodetector elements is compared with a threshold, the presence of an intercepted signal can be determined. Thus, in principle, an acousto-optical system can detect hostile communications, estimate their frequencies, and find their directions.

#### 3.4 Instantaneous Frequency Measurement

The instantaneous frequency measurement (IFM) receiver, illustrated in figure 10, is often used to estimate radar frequencies. It is possible to use it as a supplementary frequency estimator for communications, but usually not by itself. Its operation is based on the relationship among carrier frequency, path length, and phase shift of a signal. Suppose that, after passage through the bandpass filter of bandwidth  $W$ , an intercepted signal has the form

$$s(t) = A(t) \cos [\omega_0 t + \phi(t)] , \quad (102)$$

<sup>8</sup>R. A. Coppock, R. F. Croce, W. L. Regier, *Bragg Cell RF Signal Processing, Microwave J. (September 1978)*, 62.

where  $A(t)$  is the amplitude modulation and  $\phi(t)$  is the angle modulation function. As shown in figure 10, this signal is delayed by time  $\delta$  in one branch relative to the other branch. If  $\delta$  is sufficiently small, then  $A(t - \delta) \approx A(t)$  and  $\phi(t - \delta) \approx \phi(t)$  for most of the time. It follows that

$$s_1(t) \approx A(t) \cos [\omega_0 t + \phi(t) - \omega_0 \delta] \quad (103)$$

$$A(t - \delta) \approx A(t) \quad , \quad \phi(t - \delta) \approx \phi(t).$$

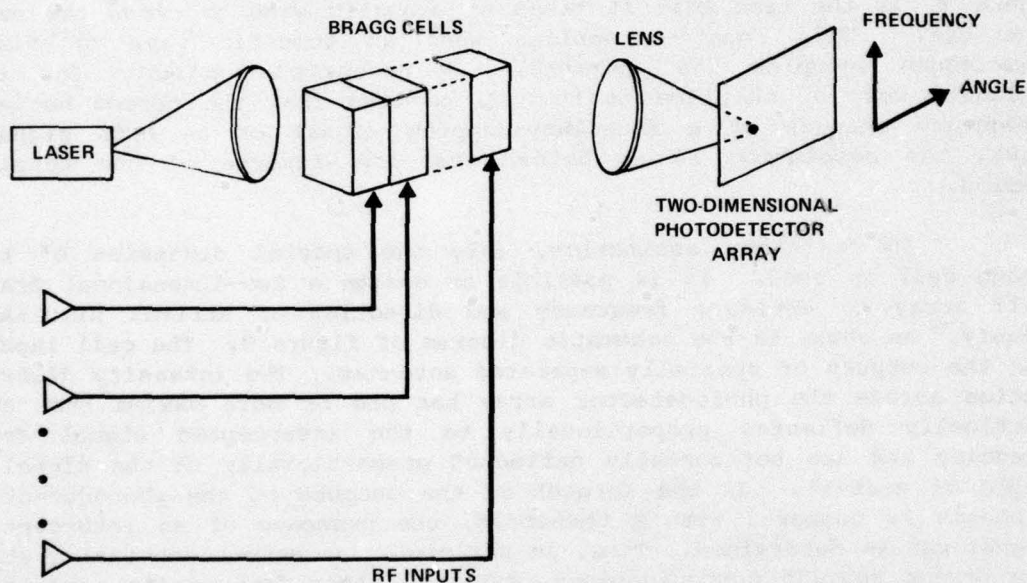


Figure 9. Array of Bragg cells for simultaneous frequency estimation and direction finding.

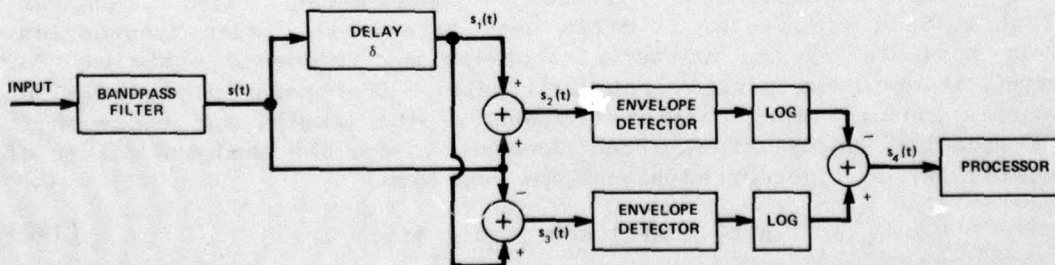


Figure 10. Instantaneous frequency measurement receiver.

By trigonometric identities, the outputs of the sum and difference operations in the figure are found to be

$$s_2(t) = \left[ 2A(t) \cos\left(\frac{\omega_0 \delta}{2}\right) \right] \cos \left[ \omega_0 t + \phi(t) - \frac{\omega_0 \delta}{2} \right] , \quad (104)$$

$$s_3(t) = \left[ 2A(t) \sin\left(\frac{\omega_0 \delta}{2}\right) \right] \sin \left[ \omega_0 t + \phi(t) - \frac{\omega_0 \delta}{2} \right] \quad (105)$$

for most of the time. The envelope detectors produce the magnitudes of the first factors in equations (104) and (105). These signals pass through logarithmic amplifiers, and the difference is taken. Thus, if  $\omega_0 \delta < \pi$ , the processor input is proportional to

$$s_4(t) = \log \tan \omega_0 \delta . \quad (106)$$

Since the modulation effects have been removed and  $\delta$  is known, the processor can calculate an estimate of  $f_0 = \omega_0/2\pi$ . The tangent function has an unambiguous inverse only over a range of  $\pi$  radians. Thus, for unambiguous operation over the frequency range of  $W$  hertz, we must have  $\delta \leq 1/2W$ . A major problem with the IFM receiver is that the resolution is inversely proportional to  $\delta$ . Since  $\delta$  must be sufficiently small so that equation (103) is valid for most of the time, the resolution may be inadequate. Another problem is that the IFM receiver cannot handle two or more simultaneously intercepted signals of comparable magnitudes.

### 3.5 Scanning Superheterodyne Receiver

Figure 11 shows a block diagram of a realization of a scanning superheterodyne receiver for frequency estimation. To explain the operation, we consider the system response to one scan of the local oscillator and an input that has constant amplitude, frequency, and phase over the scan period,  $T$ . The input is represented by

$$s(t) = A \cos(\omega_0 t + \theta) , \quad 0 \leq t \leq T , \quad (107)$$

where  $\omega_0$  is the carrier frequency and  $\theta$  is the phase angle at  $t = 0$ , which defines the beginning of the scan. The scanning waveform, which is the output of a swept local oscillator, is proportional to

$$y(t) = \cos \left( \omega_s t - \pi \mu t^2 \right) , \quad 0 \leq t \leq T , \quad (108)$$

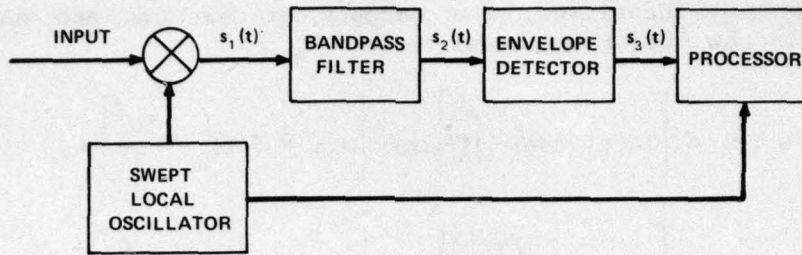


Figure 11. Scanning superheterodyne receiver.

where  $\omega_s$  is the frequency at  $t = 0$  and  $\mu$  is the scan rate, which is the rate of frequency change. The output of the mixer,  $s_1(t) = s(t)y(t)$ , passes through a bandpass filter with impulse response  $h(t)$  and bandwidth  $2B$ . Ignoring a high-frequency term that is suppressed by the bandpass filter, we have

$$s_1(t) = \frac{1}{2} A \cos(\omega_1 t + \pi \mu t^2 + \theta), \quad 0 \leq t \leq T, \quad (109)$$

where  $\omega_1 = \omega_0 - \omega_s$ .

The symmetrical bandpass filter has transfer function  $H(\omega)$  that can be written as

$$H(\omega) = H_1(\omega - \omega_c) + H_1(\omega + \omega_c), \quad (110)$$

where  $H_1(\omega)$  is the transfer function of a lowpass filter and  $\omega_c$  is the center frequency of the bandpass filter. The first term on the right side has significant values only for positive frequencies, while the second term has significant values only for negative frequencies. If  $h_1(t)$  is the impulse response of the lowpass filter, then

$$h(t) = 2h_1(t) \cos \omega_c t. \quad (111)$$

The output of the bandpass filter is

$$s_2(t) = \int_{-\infty}^{\infty} s_1(\tau) h(t - \tau) d\tau. \quad (112)$$

By using equations (109) and (111) and the pertinent trigonometric relations, equation (112) becomes

$$s_2(t) = \frac{A}{2} \int_0^T h_1(t - \tau) \cos \left[ (\omega_1 - \omega_c) \tau + \pi \mu \tau^2 + \theta + \omega_c t \right] d\tau \quad (113)$$

$$+ \frac{A}{2} \int_0^T h_1(t - \tau) \cos \left[ (\omega_1 + \omega_c) \tau + \pi \mu \tau^2 + \theta - \omega_c t \right] d\tau .$$

It is assumed that  $H_1(\omega)$  has a sufficiently narrow bandwidth that the second integral on the right side of this equation is negligible. The time-frequency diagram of figure 12, in which  $f = \omega/2\pi$ , illustrates the effect of the filter. The filter output,  $s_2(t)$ , is significant only over a portion of the scan period. Thus, we can extend the limits of the first integral to  $\pm\infty$  with negligible error if  $f_1 + \mu T > f_c + B/2$  and  $f_1 < f_c - B/2$ . Under these assumptions,

$$s_2(t) = \frac{A}{2} \int_{-\infty}^{\infty} h_1(t - \tau) \cos (\omega_2 \tau + \pi \mu \tau^2 + \theta_1) d\tau , \quad (114)$$

where  $\omega_2 = \omega_0 - \omega_s - \omega_c$  and  $\theta_1 = \theta + \omega_c t$ . To further simplify equation (114), we assume a Gaussian bandpass filter; that is,

$$H_1(\omega) = \exp \left( -\frac{\omega^2}{4a^2} - j\omega\delta \right) , \quad (115)$$

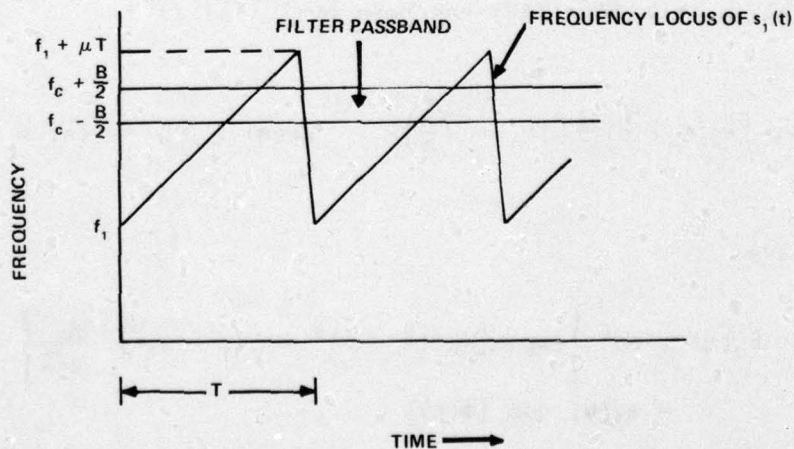


Figure 12. Time-frequency diagram for scanning superheterodyne receiver.

where parameter  $a$  is proportional to the bandwidth and  $\delta$  is the filter delay. If  $\delta$  is sufficiently large, equation (115) approximates a realizable filter. The corresponding impulse response is

$$h_1(t) = \frac{1}{2\pi} \int_{-\infty}^{\infty} H_1(\omega) e^{i\omega t} d\omega = \frac{a}{\sqrt{\pi}} \exp[-a^2(t - \delta)^2] \quad (116)$$

Substituting equation (116) into equation (114), expressing the cosine in terms of complex exponentials, and simplifying the result, we obtain

$$s_2(t) = \text{Re} \left\{ \frac{Aa}{2\sqrt{\pi}} \exp[-a^2(t - \delta)^2 + j\theta_1 + sc^2] \right. \\ \left. \times \int_{-\infty}^{\infty} \exp[-s(\tau + c)^2] d\tau \right\}, \quad (117)$$

where  $\text{Re}(x)$  denotes the real part of  $x$  and

$$s = a^2 - j\pi\mu, \quad (118) \\ c = \frac{-2a^2(t - \delta) - j\omega_2}{2s}.$$

The integral in equation (117) has been evaluated as<sup>5</sup>

$$\int_{-\infty}^{\infty} \exp[-s(\tau + c)^2] d\tau = \left(\frac{\pi}{s}\right)^{1/2}, \quad \text{Re}(s) \geq 0, \quad \text{Re}(\sqrt{s}) > 0. \quad (119)$$

Thus, we have

$$s_2(t) = \text{Re} \left\{ \exp[-a^2(t - \delta)^2 + j\theta_1 + sc^2] \frac{Aa}{2\sqrt{s}} \right\} \\ = s_3(t) \cos[\phi(t)], \quad (120)$$

<sup>5</sup>A. Papoulis, *Signal Analysis*, McGraw-Hill Book Co., New York (1977).



where

$$\phi(t) = \frac{4\pi a^4 \mu (t - \delta)^2 + 4a^4 \omega_2 (t - \delta) - \pi \mu \omega_2^2}{4(a^4 + \pi^2 \mu^2)} + \theta_1 + \frac{1}{2} \tan^{-1} \left( \frac{\pi \mu}{a^2} \right)$$

$$s_3(t) = \frac{A}{2} \left( 1 + \frac{\pi^2 \mu^2}{a^4} \right)^{-1/4} \exp \left[ - \frac{a^2 (2\pi \mu t - 2\pi \mu \delta + \omega_2^2)}{4(a^4 + \pi^2 \mu^2)} \right] . \quad (121)$$

As indicated in figure 11,  $s_2(t)$  is applied to an envelope detector that extracts the envelope,  $s_3(t)$ , from the input. The peak value of  $s_3(t)$  is attained when  $t = \delta - (\omega_2/2\pi\mu) = \delta - (f_0 - f_s - f_c)/\mu$ . Thus, the input frequency  $f_0$  can easily be estimated from the time location of the peak value. The normalized peak value,  $\alpha$ , which is defined as the peak value relative to  $A/2$ , the peak value for small  $\mu$ , is

$$\alpha = \left( 1 + \frac{\pi^2 \mu^2}{a^4} \right)^{-1/4} . \quad (122)$$

The half-power points of  $s_3(t)$  are determined by setting the exponential factor in equation (121) equal to  $1/\sqrt{2}$ . The pulse duration of  $s_3(t)$  between half-power points is determined to be

$$T_p = \frac{a(2 \ln 2)^{1/2}}{\pi \mu} \left( 1 + \frac{\pi^2 \mu^2}{a^4} \right)^{1/2} . \quad (123)$$

The frequency resolution in hertz,  $\Delta$ , as determined by the processor of figure 11, is approximately equal to  $\mu T_p$ , the frequency range scanned during pulse duration  $T_p$ . Thus, the resolution is

$$\Delta = \frac{a(2 \ln 2)^{1/2}}{\pi} \left( 1 + \frac{\pi^2 \mu^2}{a^4} \right)^{1/2} . \quad (124)$$

From equation (115), the 3-dB power spectrum bandwidth in hertz is related to parameter  $a$  by

$$B = \frac{(2 \ln 2)^{1/2}}{\pi} a . \quad (125)$$

In terms of B, we can write

$$\alpha = \left( 1 + 0.195 \frac{\mu^2}{B^4} \right)^{-1/4}, \quad (126)$$

$$\Delta = B \left( 1 + 0.195 \frac{\mu^2}{B^4} \right)^{1/2}. \quad (127)$$

These equations were originally derived for the theory of spectrum analyzers.<sup>9</sup>

If the scan rate,  $\mu$ , is high,

$$\alpha \approx 1.5 \frac{B}{\sqrt{\mu}}, \quad \Delta \approx 0.44 \frac{\mu}{B}, \quad \mu \gg B^2, \quad (128)$$

which clearly show the effects of increasing  $\mu$ .

Using elementary calculus, we determine the optimal filter bandwidth,  $B_0$ , to minimize  $\Delta$ . Substituting this value of  $B_0$  into equation (127), we obtain  $\Delta_0$ , the minimum resolution as a function of  $\mu$ . The results are

$$B_0 = 0.664\sqrt{\mu}, \quad \Delta_0 = \sqrt{2} B_0. \quad (129)$$

The corresponding normalized peak value is

$$\alpha_0 = 0.84, \quad (130)$$

which is no longer a function of  $\mu$ . If the optimal bandwidth is used, these equations indicate that the achievable resolution becomes worse as  $\mu$  increases, but the peak value does not change.

---

<sup>9</sup>M. Engelson and F. Telewski, *Spectrum Analyzer Theory and Applications*, Artech House, Inc., Dedham, MA (1974).

### 3.6 Microscan Receiver

Improved resolution at a high scan rate can be achieved by a microscan receiver, which uses the compression of pulses. The microscan receiver (fig. 13a) includes a dispersive filter, whereas the scanning superheterodyne receiver includes a bandpass filter.

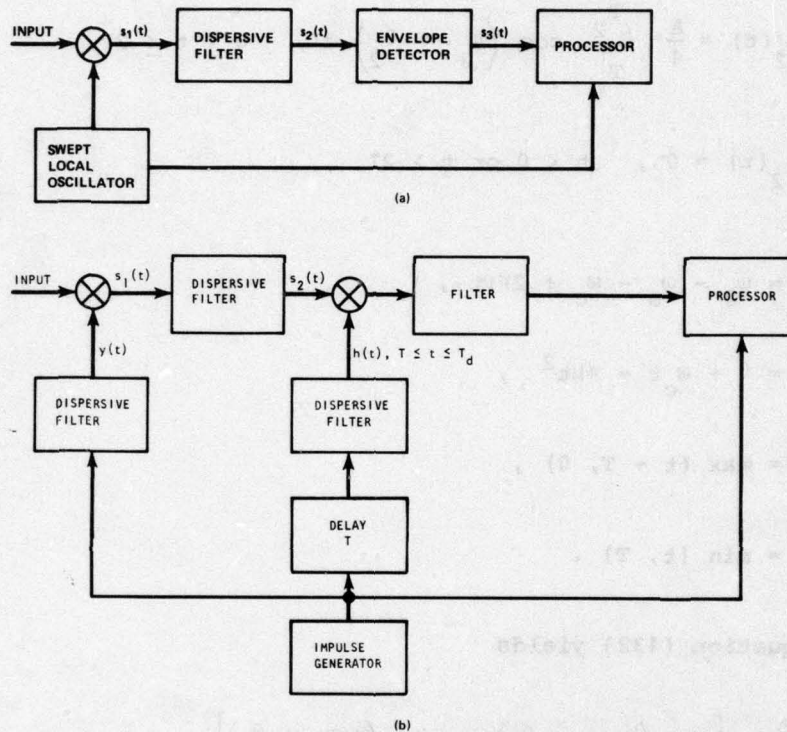


Figure 13. Microscan receivers for (a) frequency estimation or magnitude of Fourier transform and (b) real part of Fourier transform.

The impulse response of the dispersive filter is modeled as

$$h(t) = \cos(\omega_c t - \pi \mu t^2), \quad 0 \leq t \leq T_d, \quad (131)$$

where  $T_d$  is the duration of the impulse response and the amplitude has been normalized to unity. The dispersive filter can be realized by a surface acoustic wave device.<sup>10</sup> Substituting this equation and equation (109) into equation (112) yields the dispersive filter response to one

<sup>10</sup>A. A. Oliner, ed., *Acoustic Surface Waves*, Springer-Verlag New York, Inc., New York (1978).

scan of the local oscillator and an input represented by equation (107) over the scan period. Initially, we set  $T_d = T$ . Using  $2 \cos u \cos v = \cos(u - v) + \cos(u + v)$ , we may write the result as the sum of the two integrals. We assume that  $|\omega_0 - \omega_s - \omega_c| \ll |\omega_0 - \omega_s + \omega_c|$  so that, for most values of  $t$ , we may neglect one of the integrals. We are left with the approximation

$$s_2(t) = \frac{A}{4} \int_{T_1}^{T_2} 2 \cos(\omega_3 \tau + \theta_2) d\tau, \quad 0 \leq t \leq 2T,$$

$$s_2(t) = 0, \quad t < 0 \text{ or } t > 2T, \quad (132)$$

where

$$\omega_3 = \omega_0 - \omega_s - \omega_c + 2\pi\mu t,$$

$$\theta_2 = \theta + \omega_c t - \pi\mu t^2, \quad (133)$$

$$T_1 = \max(t - T, 0),$$

$$T_2 = \min(t, T).$$

If  $\omega_3 \neq 0$ , equation (132) yields

$$s_2(t) = \frac{A}{4\omega_3} \left[ \sin(\omega_3 T_2 + \theta_2) - \sin(\omega_3 T_1 + \theta_2) \right] \quad (134)$$

$$= \frac{A}{2\omega_3} \sin \left[ \frac{\omega_3}{2} (T_2 - T_1) \right] \cos \left[ \frac{\omega_3}{2} (T_1 + T_2) + \theta_2 \right].$$

The final form of equation (134) is valid even if  $\omega_3 = 0$ . For practical values of the parameters, the cosine factor varies much more rapidly with time than other factors. Consequently, using equations (133), the output of the envelope detector is

$$s_3(t) = \frac{At}{4} \operatorname{sinc} \left[ (f_0 - f_s - f_c) t + \mu t^2 \right], \quad 0 \leq t \leq T, \quad (135)$$

$$s_3(t) = \frac{A(2T - t)}{4} \operatorname{sinc} \left[ (f_0 - f_s - f_c + \mu t) (2T - t) \right], \quad T \leq t \leq 2T,$$

where we have set  $\omega = 2\pi f$ .

The peak value of  $s_3(t)$  is  $AT/4$ . We define parameter  $\epsilon$  as

$$\epsilon = f_s + f_c - f_0 - \mu T. \quad (136)$$

If the frequency of the intercepted signal is such that  $\epsilon = 0$ , then the peak value of  $s_3(t)$  occurs at  $t = T$ ; that is,

$$s_3(T) = \frac{AT}{4}, \quad \epsilon = 0. \quad (137)$$

We also have

$$s_3\left(T \pm \frac{1}{2\mu T}\right) \approx \frac{AT}{4} (0.64), \quad \epsilon = 0, \quad T \gg \frac{1}{\mu T}, \quad (138)$$

$$s_3\left(T \pm \frac{1}{\mu T}\right) \approx 0, \quad \epsilon = 0, \quad T \gg \frac{1}{\mu T}.$$

These equations indicate that  $1/\mu T$  is an approximate measure of the width of the compressed output pulse. Satisfying the inequality ensures that the response of the microscan receiver due to one scan does not interact significantly with the response due to the next scan.

If the frequency of the intercepted signal shifts slightly, then  $\epsilon \neq 0$ . A small shift yields

$$s_3\left(T + \frac{\epsilon}{\mu}\right) \approx \frac{AT}{4}, \quad \left|\frac{\epsilon}{\mu}\right| \ll T, \quad (139)$$

where the right side of the equation is the peak value of  $s_3(t)$ . Thus, the peak value occurs at time  $t = T + \epsilon/\mu$ . Using equation (136), we can estimate the input frequency,  $f_0 = \omega_0/2\pi$ , from the time location of the peak value.

We define the resolution of the microscan receiver,  $\Delta$ , as the value of the frequency shift in hertz,  $\epsilon$ , that produces a shift in the time of the peak output equal to the width of the output when  $\epsilon = 0$ . Thus,

$$\Delta = \frac{1}{T} = \frac{\mu}{W}. \quad (140)$$

where  $W = \mu T$  is the total bandwidth scanned.

The ratio of the input pulse width to the compressed output pulse width is  $TW$ , which is called the compression ratio of the microscan receiver. When this ratio is large, a comparison of equations (140) and (129) indicates that there is a substantial improvement in resolution of the microscan receiver over the scanning superheterodyne receiver. A comparison of the receiver outputs for typical inputs of the form of equation (107) is depicted in figure 14.

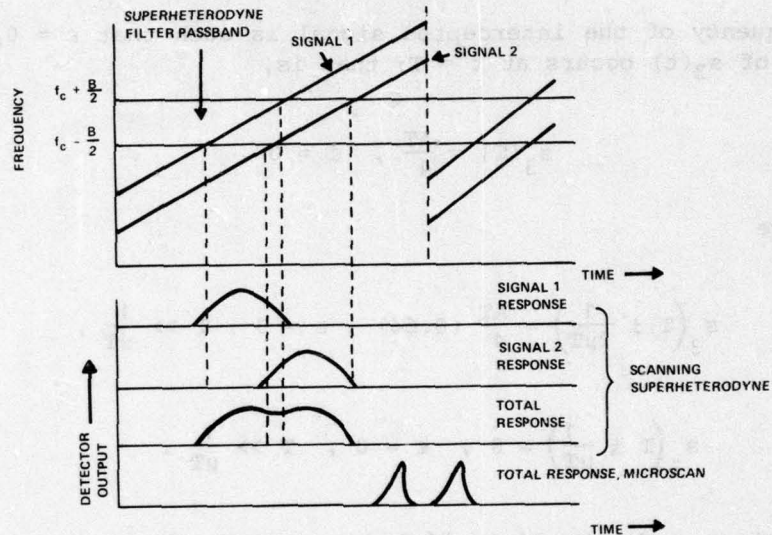


Figure 14. Response of scanning superheterodyne and microscan receivers to simultaneous signals.

Due to the presence of the sinc function, equation (135) exhibits smaller subsidiary peaks in addition to the main peak. In a multiple-target environment, these side lobes can mask adjacent main peaks due to other targets, thus limiting the frequency resolution and dynamic range of the receiver. Consequently, it is sometimes desirable to follow the dispersive filter with a shaping filter for side-lobe reduction or to modify the impulse response of the dispersive filter itself.

For a large compression ratio, the transfer function associated with equation (131) has a flat, nearly rectangular amplitude response and a quadratic phase response<sup>11</sup> over bandwidth  $W$ .

The preceding analysis is valid if the modulation period of the input is large compared with the scan period. If a more rapidly modulated input is present, the microscan receiver can be designed to

<sup>11</sup>H. J. Blinchikoff and A. I. Zverev, *Filtering in the Time and Frequency Domains*, John Wiley and Sons, Inc., New York (1976).

produce an output that is an approximation of the Fourier transform of the modulation. In this case, the system is often called a chirp transform processor. As previously, we consider the system response to one scan of the local oscillator. Over the scan period, the input is assumed to have the form

$$s(t) = s_0(t) \cos(\omega_0 t + \theta), \quad 0 \leq t \leq T. \quad (141)$$

This input is mixed with the scanning waveform of equation (108) to produce

$$s_1(t) = \frac{1}{2} s_0(t) \cos(\omega_1 t + \pi \mu t^2 + \theta), \quad 0 \leq t \leq T. \quad (142)$$

The impulse response of the dispersive filter is given by equation (131), where we assume that  $T_d \geq T$ . We calculate the system output in the time interval  $T \leq t \leq T_d$ . Substituting equations (142) and (131) into equation (112), using trigonometry, dropping a negligible integral, and substituting a complex exponential, we obtain

$$\begin{aligned} s_2(t) &= \operatorname{Re} \left\{ \frac{1}{4} \exp \left[ j(\omega_c t - \pi \mu t^2 + \theta) \right] \int_{-\infty}^{\infty} s_0(\tau) q(\tau) \exp \left[ -j\tau(\omega_c - \omega_1 - 2\pi \mu t) \right] d\tau \right\} \\ &= \operatorname{Re} \left\{ \frac{1}{4} \exp \left[ j(\omega_c t - \pi \mu t^2 + \theta) \right] S_0(\omega_c - \omega_1 - 2\pi \mu t) \right\} \\ &= \frac{1}{4} |S_0(\omega_c - \omega_1 - 2\pi \mu t)| \cos \left[ \omega_c t - \pi \mu t^2 + \theta + \phi(\omega_c - \omega_1 - 2\pi \mu t) \right], \\ & \quad T \leq t \leq T_d, \end{aligned} \quad (143)$$

where  $q(t)$  is defined in equation (85),  $S_0(\omega)$  is the Fourier transform of  $s_0(\tau)q(\tau)$ , and  $\phi(\omega)$  is the phase angle of the Fourier transform. The output of the envelope detector is proportional to

$$s_3(t) = |S_0(\omega_s + \omega_c - \omega_0 - 2\pi \mu t)|, \quad T \leq t \leq T_d. \quad (144)$$

Thus, the magnitude of the Fourier transform of the input modulation has been produced as a time signal.

If  $s_2(t)$  is multiplied by  $h(t)$ , then equations (131) and (143) indicate that, after elimination of a double frequency term by filtering, the phase-shifted real part of  $S_0(\omega)$  is produced as a time signal. As shown in figure 13(b) the waveform  $h(t)$ ,  $T \leq t \leq T_d$ , can be produced by applying an impulse at time  $T$  to a dispersive filter with impulse response  $h_1(t) = h(t + T)$ ,  $0 \leq t \leq T_d - T$ . The phase-shifted imaginary part of  $S_0(\omega)$  can be produced as a time signal by multiplying  $s_2(t)$  by  $\sin(\omega_c t - \pi \mu t^2)$ .

Let  $\omega_m$  denote the maximum value of  $\omega$  for which  $|S_0(\omega)|$  has a significant value. If

$$T + \frac{\omega_m}{2\pi\mu} \leq \frac{\omega_s + \omega_c - \omega_0}{2\pi\mu} \leq T_d, \quad (145)$$

then during the time interval  $T \leq t \leq T_d$ ,  $s_3(t)$  exhibits all the values of  $|S_0(\omega)|$  for  $0 \leq \omega \leq \omega_m$ . The range of possible values of  $f_0 = \omega_0/2\pi$  for which equation (145) can be satisfied is

$$W_R = \mu T_d - f_m - \mu T, \quad T_d \geq T + \frac{f_m}{\mu}, \quad (146)$$

where  $f_m = \omega_m/2\pi$ . If we wish to avoid the interference of the Fourier transform generated by a scan, which occurs during  $T \leq t \leq T_d$ , with the Fourier transform generated by the next scan, then we set  $T_d \leq 2T$ . In terms of the total bandwidth scanned,  $W = \mu T$ , we have

$$0 \leq W_R \leq W \left(1 - \frac{f_m}{W}\right), \quad T + \frac{f_m}{\mu} \leq T_d \leq 2T. \quad (147)$$

If  $f_m \ll W$  and  $T_d = 2T$ , then  $W_R \approx W$ .

The inequality for  $T_d$  in equation (147) is necessary for satisfactory spectral analysis. However, for frequency estimation alone, setting  $T_d = T$  not only is adequate, but also minimizes the interference between scan responses.

The chirp transform processor can be used as the basic building block of an analog version of the cross correlator of figure 5.

In addition to frequency estimation, the microscan receiver can be used for detection. Alternatively, if interception is verified by a parallel system designed expressly for that purpose, frequency can be estimated by the microscan receiver.



If the scanning period is less than the period between frequency changes of the intercepted signal, the microscan and scanning superheterodyne receivers can estimate each frequency of a frequency-hopping or MFSK signal. If not, some frequencies may be missed, and the estimation accuracy is degraded. The inherent linearity of these two receivers makes them potentially effective in analyzing many simultaneous intercepted signals.

#### 4. DIRECTION FINDING

Signals must be detected, and sometimes the frequency must be estimated, if direction is to be found. Conversely, direction finding provides signal sorting, which restricts the number of signals that the detection and frequency estimation systems must process simultaneously.

For simplicity, the estimation of a single bearing angle is considered. In a ground-based interception system, an azimuth angle may be all that is needed. However, airborne systems may require estimates of both the azimuth and the elevation angles to the intercepted transmitter.

##### 4.1 Energy Comparison Systems

Energy comparison systems are analogous to the amplitude comparison systems used in radar<sup>12</sup>, but when communications with unknown parameters are to be intercepted, it is logical to base comparisons upon the energy rather than the amplitude. The stationary multibeam system for direction finding is illustrated in figure 15. First, the largest of the receiver outputs is selected. Next, the larger of the two receiver outputs corresponding to beams adjacent to the beam that produced the largest output is selected. The two selected outputs are denoted by  $L_1$  and  $L_2$ . The processor compares the outputs to a threshold for detection. The angle of arrival is estimated from the logarithm of the ratio of  $L_1$  to  $L_2$ . The radiation patterns of the adjacent beams are illustrated in figure 16, where  $\phi$  represents the angle of arrival of an intercepted signal, and beam pattern  $F_1(\theta)$  produces  $L_1$ . The origin of the coordinate system is defined so that  $+\psi$  and  $-\psi$  indicate the peak responses of the two beams, respectively. Suppose that the beam patterns are approximately Gaussian; that is, they are described by

$$F_1(\theta) = K_1 \exp \left[ -\frac{(\theta - \psi)^2}{b^2} \right], \quad (148)$$

<sup>12</sup>D. K. Barton, *Radar System Analysis*, Artech House, Inc., Dedham, MA (1976).

$$F_2(\theta) = K_2 \exp \left[ -\frac{(\theta + \psi)^2}{b^2} \right], \quad (149)$$

where  $K_1$  and  $K_2$  are constants independent of  $\theta$ , and  $b$  is a measure of the beam width. If the receivers contain radiometers, then the  $L_i$  are proportional to the squares of the  $F_i$ . Thus, in the absence of noise, the processor input is

$$Z = \ln \frac{L_1(\phi)}{L_2(\phi)} = 2 \ln \frac{K_1}{K_2} + \frac{8\psi\phi}{b^2}. \quad (150)$$

The angle of arrival can be determined by inverting this equation. In the presence of noise, the same inverse provides an estimate,  $\hat{\phi}$ , of the actual angle  $\phi$ . We have

$$\hat{\phi} = \frac{b^2}{8\psi} \left( Z - 2 \ln \frac{K_1}{K_2} \right), \quad (151)$$

where  $Z$  is now a random variable. Since  $\hat{\phi}$  is a linear function of  $Z$ , the required processing is quite simple. We give an error analysis assuming that  $L_1$  and  $L_2$  are correctly chosen.

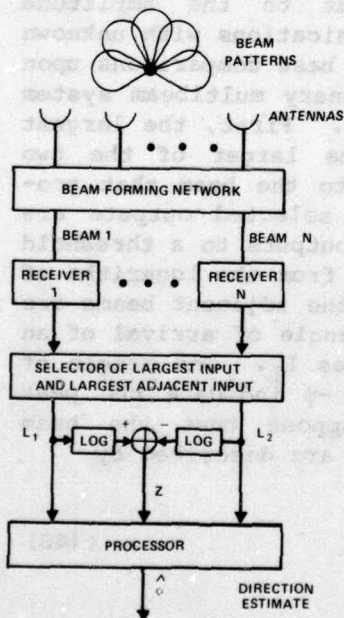


Figure 15. Stationary multibeam system.

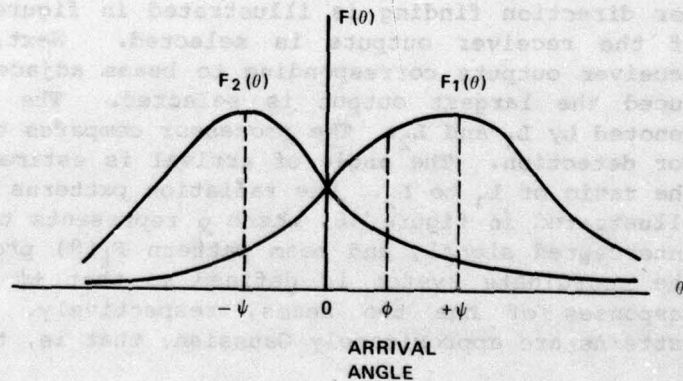


Figure 16. Adjacent antenna radiation patterns.

Because  $L_1$  and  $L_2$  are the outputs of radiometers, they are statistically independent, noncentral  $\chi^2$  random variables with  $\gamma$  degrees of freedom and noncentral parameters  $\lambda_1$  and  $\lambda_2$ , respectively. From elementary probability theory, the probability density function of  $Y = L_1/L_2$ , the quotient of two nonnegative random variables, is

$$p_2(y) = \int_0^{\infty} x p_{11}(yx) p_{12}(x) dx, \quad y \geq 0, \quad (152)$$

$$p_2(y) = 0, \quad y < 0,$$

where  $p_{11}(x)$  and  $p_{12}(x)$  are the density functions for  $L_1$  and  $L_2$ , respectively. The density function  $p_{1i}(x)$  is given by equation (30) with  $\lambda_i$  substituted for  $\lambda$ . The noncentral parameters are given by

$$\lambda_1 = \frac{2E_1}{N_0} \exp \left[ -\frac{2(\phi - \psi)^2}{b^2} \right],$$

$$\lambda_2 = \frac{2E_2}{N_0} \exp \left[ -\frac{2(\phi + \psi)^2}{b^2} \right], \quad (153)$$

where  $E_i$  is the energy received when the intercepted signal enters the center of the beam associated with  $L_i$ .

From equations (151) to (153) and the fact that  $Z = \ln Y$ , we can determine the root-mean-square error of  $\hat{\phi}$ , which we denote by  $E_R$ . By definition and a straightforward expansion,

$$E_R^2 = E [(\hat{\phi} - \phi)^2] = \text{VAR}(\hat{\phi}) + B_\phi^2, \quad (154)$$

where  $\text{VAR}(\hat{\phi})$  is the variance of  $\hat{\phi}$  and  $B_\phi$  is the bias,

$$B_\phi = E[\hat{\phi}] - \phi. \quad (155)$$

To evaluate  $E_R$ , we need the first two moments of  $Z$ . For simplicity, we assume that  $K_1 = K_2$  and  $E_1 = E_2$ . When  $\phi = 0$ , equations (153) give  $\lambda_1 = \lambda_2$  so that  $L_1$  and  $L_2$  are identically distributed random variables.

Since  $Z = \ln L_1 - \ln L_2$ , it follows that

$$E[Z] = 0, \quad \phi = 0. \quad (156)$$

At other values of  $\phi$ , closed-form expressions for the mean and other moments are difficult to obtain. In general, the distribution of  $L_1$  at  $\phi$  is identical to the distribution of  $L_2$  at  $-\phi$ . Thus,  $E_R$  is symmetric about  $\phi = 0$ .

To obtain an approximate expression for  $E[Z]$ , we write the integral for  $E[\ln Y]$  as a double integral and change coordinates:

$$\begin{aligned} E[Z] &= \int_0^\infty \int_0^\infty x \ln y p_{11}(yx) p_{12}(x) dx dy \\ &= \int_0^\infty \int_0^\infty \ln\left(\frac{v}{x}\right) p_{11}(v) p_{12}(x) dx dv. \end{aligned} \quad (157)$$

The logarithm is approximated by the first six terms of its two-dimensional Taylor series expansion about the point  $v = m_1$ ,  $x = m_2$ , where  $m_1$  and  $m_2$  are the mean values of  $L_1$  and  $L_2$ , respectively. Thus,

$$\begin{aligned} \ln\left(\frac{v}{x}\right) &\approx \ln\left(\frac{m_1}{m_2}\right) + \frac{v - m_1}{m_1} - \frac{x - m_2}{m_2} - \frac{(v - m_1)^2}{2m_1^2} \\ &\quad + \frac{(x - m_2)^2}{2m_2^2} - \frac{(v - m_1)(x - m_2)}{2m_1 m_2}. \end{aligned} \quad (158)$$

This approximation is accurate over some range of  $v$  and  $x$  about  $v = m_1$ ,  $x = m_2$ . If  $p_{11}(v)$  and  $p_{12}(x)$  are negligible outside this range, then the substitution of equation (158) into equation (157) yields an accurate approximation of  $E[Z]$ . The ranges of significant values of  $p_{11}(v)$  and  $p_{12}(x)$  are approximately limited by  $|v - m_1| < 3\sigma_1$  and  $|x - m_2| < 3\sigma_2$ , where  $\sigma_1$  and  $\sigma_2$  are the standard deviations of  $L_1$  and  $L_2$ , respectively. Thus, sufficient conditions for the valid use of equation (158) are  $\sigma_1 \ll m_1$  and  $\sigma_2 \ll m_2$ .

Making the substitution and using the properties of density functions, we obtain

$$E[Z] \approx \ln\left(\frac{m_1}{m_2}\right) - \frac{\sigma_1^2}{2m_1^2} + \frac{\sigma_2^2}{2m_2^2}, \quad \sigma_1 \ll m_1, \quad \sigma_2 \ll m_2. \quad (159)$$

From equations (26) and (27), we have

$$m_i = \lambda_i + 2\gamma, \quad i = 1, 2, \quad (160)$$

$$\sigma_i^2 = 4\lambda_i + 4\gamma, \quad i = 1, 2. \quad (161)$$

An approximate expression for  $E[Z^2]$  is obtained in an analogous manner. Combining this expression with equation (159) and dropping terms higher than second order in  $\sigma_1/m_1$  and  $\sigma_2/m_2$ , we obtain

$$\text{VAR}(Z) \approx \frac{\sigma_1^2}{m_1^2} + \frac{\sigma_2^2}{m_2^2}, \quad \sigma_1 \ll m_1, \quad \sigma_2 \ll m_2. \quad (162)$$

By using  $K_1 = K_2$  and equations (151), (154), (159), and (162), an equation for  $E_R$  can be derived,

$$E_R = \frac{b^2}{8\psi} \left\{ \frac{\sigma_1^2}{m_1^2} + \frac{\sigma_2^2}{m_2^2} + \left[ \ln\left(\frac{m_1}{m_2}\right) - \frac{\sigma_1^2}{2m_1^2} + \frac{\sigma_2^2}{2m_2^2} - \frac{8\psi\phi}{b^2} \right]^2 \right\}^{1/2},$$

$$\sigma_1 \ll m_1, \quad \sigma_2 \ll m_2. \quad (163)$$

Figures 17 and 18 show representative plots of  $E_R$  versus  $\phi$ . Figure 17 illustrates the effect of the normalized beam width,  $b/\psi$ , on  $E_R$ . For  $E/N_0 = 10^4$ ,  $\gamma = 10^3$ , and  $\phi = \psi$  the normalized beam width that minimizes  $E_R$  is approximately 4.5. However, the curves show that this normalized beam width is not optimal for other values of  $\phi$ . Figure 18 illustrates the effect of increasing the observation interval,  $T$ . Since an increase in  $T$  causes proportionate increases in  $E$  and  $\gamma$ , we set  $E/N_0 = 10\gamma$  for each value of  $\gamma$ . The optimal normalized beam width for each value of  $\gamma$  and  $\phi = \psi$  is chosen. The curves show a steady decrease in  $E_R$  as  $\gamma$  increases.

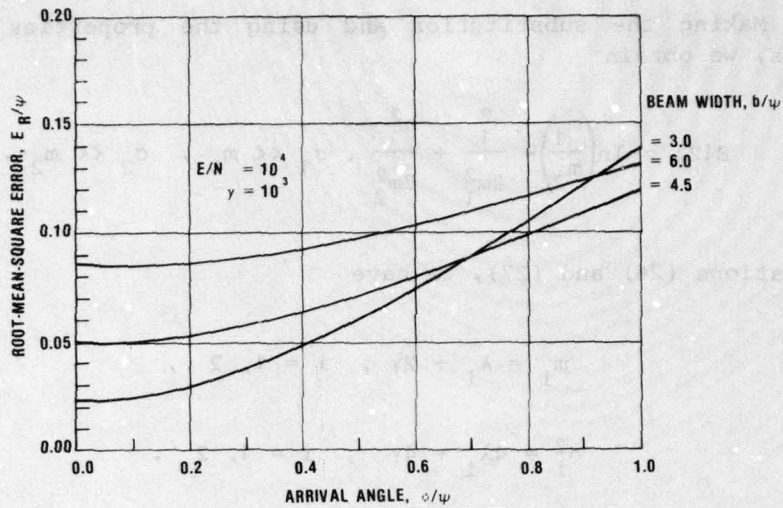


Figure 17. Root-mean-square error versus arrival angle for different beam widths.

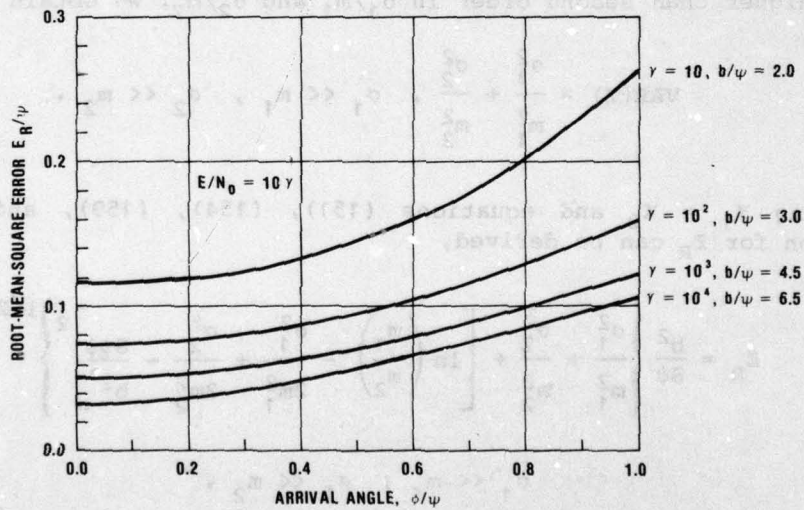


Figure 18. Root-mean-square error versus arrival angle for optimal beam widths and different values of  $\gamma$ .

Suppose many frequency-hopping signals are simultaneously intercepted by a channelized receiver. If it is impossible to correlate successive hopping frequencies, the direction of a signal must be estimated on the basis of the energy received in a single channel during a single hopping period. With this interpretation,  $\gamma$  is proportional to the hopping period, and figure 18 indicates the loss in directional accuracy resulting from an increase in hopping rate.

Energy comparison with a rotating beam is illustrated in figure 19. A rotating dish or an electronically scanned phased array is used with an omnidirectional antenna a small distance apart. The receivers are radiometers. Detection of a signal is verified and an estimate of direction is obtained by measuring the ratio of  $L_1$  to  $L_2$  and comparing the ratio to a threshold. Because a ratio is used, the effects of amplitude modulation and rotation can be largely eliminated by the processor. Signals entering through the side lobes and the back lobes of the rotating beam are inhibited. Alternatively, if two simultaneously rotating beams are offset relative to each other, sum and difference outputs can be produced (fig. 20), as in monopulse radar systems. If the intercepted signal duration is sufficient, the accuracy of the direction estimates of the systems of figures 19 and 20 can be improved by continued processing. After the target is detected, the rotation slows or stops. Processing over an increased observation interval allows further adjustment of antenna position until the intercepted signal's direction of arrival is fixed near the center of the rotating beam or beams.

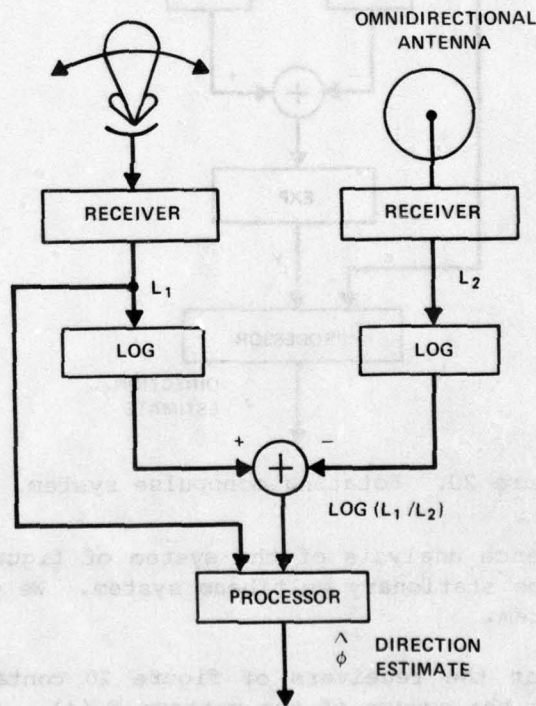


Figure 19. Rotating beam system.

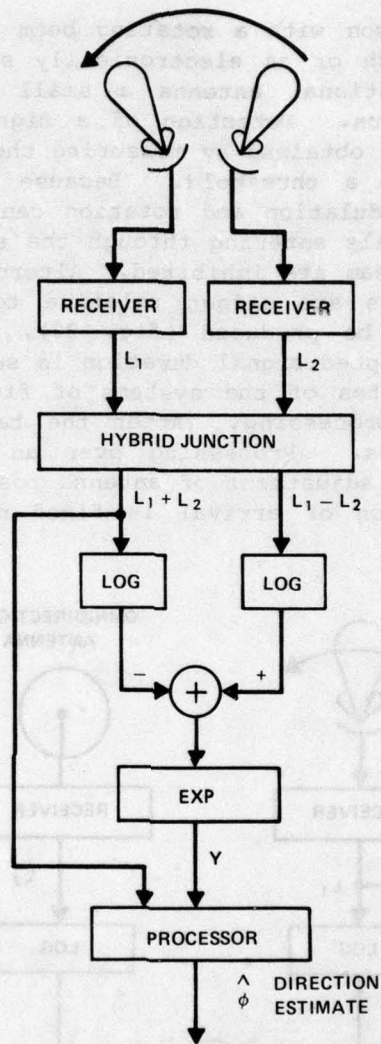


Figure 20. Rotating monopulse system.

The performance analysis of the system of figure 19 is similar to the analysis of the stationary multibeam system. We give an analysis of the monopulse system.

Assuming that the receivers of figure 20 contain radiometers,  $L_i$  is proportional to the square of the pattern  $F_i(\phi)$ . It follows that, in the absence of noise,

$$Y = \frac{L_1 - L_2}{L_1 + L_2} = \frac{F_1^2(\phi) - F_2^2(\phi)}{F_1^2(\phi) + F_2^2(\phi)}. \quad (164)$$



If the antenna beam patterns are given by equations (148) and (149) with  $K_1 = K_2$ , then

$$Y = \tanh \frac{4\psi\phi}{b^2} . \quad (165)$$

The angle of arrival can be determined by inverting equation (165). In the presence of noise, the same inversion provides an estimate of the actual angle. Near  $\phi = 0$ , the estimate is approximated by

$$\hat{\phi} \approx \frac{b^2}{4\psi} Y , \quad \phi \ll \frac{b^2}{4\psi} , \quad (166)$$

where  $Y$  is now a random variable.

The probability density function of  $Y$  is complicated. However, the first two moments of  $Y$  can be approximately determined without explicitly deriving the density. By definition,

$$E[Y^n] = \int_0^\infty \int_0^\infty \left( \frac{x-v}{x+v} \right)^n p_{11}(x) p_{12}(v) dx dv . \quad (167)$$

Proceeding in a manner analogous to the evaluation of equation (157), we derive equations for  $E[Y]$  and  $\text{VAR}(Y)$  from equation (167) with  $n = 1, 2$ . Using equations (154) and (166) and retaining only second order terms in  $\sigma_1/m_1$  and  $\sigma_2/m_2$ , we obtain

$$E_R = \frac{b^2}{4\psi} \left\{ \frac{4(m_2^2\sigma_1^2 + m_1^2\sigma_2^2)}{(m_1 + m_2)^4} + \left[ \frac{m_1 - m_2}{m_1 + m_2} - \frac{2(m_2\sigma_1^2 - m_1\sigma_2^2)}{(m_1 + m_2)^3} - \frac{4\psi\phi}{b^2} \right]^2 \right\}^{1/2} , \quad (168)$$

$$\phi \ll \frac{b^2}{4\psi} , \quad \sigma_1 \ll m_1 , \quad \sigma_2 \ll m_2 .$$

At  $\phi = 0$ , we have  $m_1 = m_2 = m$  and  $\sigma_1 = \sigma_2 = \sigma$  so that

$$E_R = \frac{\sqrt{2}b^2\sigma}{8\psi m}, \quad \phi = 0, \quad \sigma \ll m. \quad (169)$$

Appropriate substitution into this equation indicates that we can achieve  $E_R \ll b$  if the observation interval,  $T$ , is sufficiently large. Thus, the potential direction-finding accuracy is much better than a beam width.

To compare this result with the corresponding result for the stationary multibeam array, we set  $m_1 = m_2 = m$ ,  $\sigma_1 = \sigma_2 = \sigma$ , and  $\phi = 0$  in equation (163). The result is equation (169). Thus, if  $\phi = 0$ , the stationary multibeam array performs as well as the monopulse system. However, if  $\phi \neq 0$ ,  $E_R$  increases in the multibeam case. In the monopulse case, if the intercepted signal duration is sufficient, the antennas can adjust their positions until  $\phi \approx 0$  so that the  $E_R$  after adjustment is given by equation (169). The main disadvantage with the monopulse or other rotating beam system is the narrow instantaneous field of view, which may cause a signal to be missed or may decrease the possible observation time. On the other hand, when many hostile communications are present, the narrow field of view provides a valuable signal-sorting capability.

#### 4.2 Interferometer

Another direction-finding system is the interferometer, which also forms the heart of phase-comparison monopulse radar systems.<sup>12</sup> An interferometer consists of two or more antennas or groups of elements of a phased array that use phase or arrival-time information to estimate direction (fig. 21). The antennas may be rotating and directional.

We first consider the interferometer of figure 21(a). Suppose a plane wave arrives at angle  $\phi$ , where  $|\phi| \leq \pi/2$ . If two antennas are separated by distance  $d$ , then since phase angles are modulo  $2\pi$  numbers, the phase difference between the antenna outputs is

$$\theta = \frac{2\pi d \sin \phi}{\lambda_s} - 2\pi n, \quad |\theta| \leq \pi, \quad |\phi| \leq \frac{\pi}{2}, \quad (170)$$

<sup>12</sup>D. K. Barton, *Radar System Analysis*, Artech House, Inc., Dedham, MA (1976).

where  $\lambda_s$  is the signal wavelength and  $n$  is an integer that ensures satisfaction of the first inequality. If  $d \leq \lambda_s/2$ , then  $n = 0$ . If  $d > \lambda_s/2$ , then  $n$  varies with  $\phi$ , taking negative and positive values and the value zero.

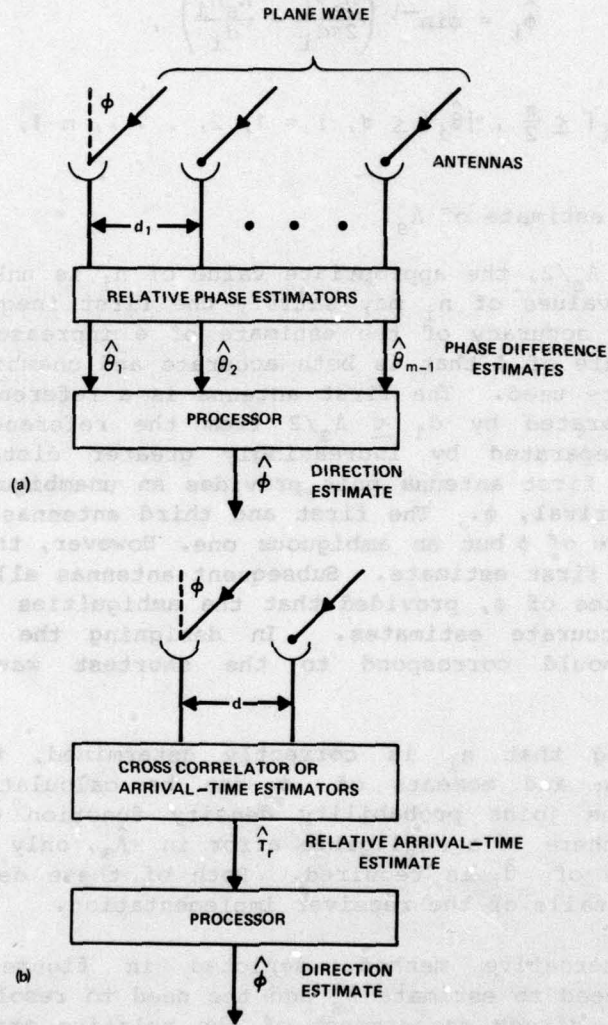


Figure 21. Interferometers using (a) phase information and (b) arrival-time information.

One antenna output provides a reference. Each of the other antenna outputs is applied to a separate device that estimates its phase relative to the reference. This device may be similar to the part of the IFM receiver in figure 10 that is fed by  $s(t)$  and  $s_1(t)$ . The estimates of the relative phases are denoted by  $\hat{\theta}_i$ .

Estimates of the angle of arrival are calculated from the  $\hat{\theta}_i$  by inverting equation (170). If there are  $m$  antennas, the  $(m - 1)$  estimates are given by

$$\hat{\phi}_i = \sin^{-1} \left( \frac{\hat{\Lambda}_s \hat{\theta}_i}{2\pi d_i} + \frac{\hat{\Lambda}_s n_i}{d_i} \right), \quad (171)$$

$$|\hat{\phi}_i| \leq \frac{\pi}{2}, \quad |\hat{\theta}_i| \leq \pi, \quad i = 1, 2, \dots, m-1,$$

where  $\hat{\Lambda}_s$  is an estimate of  $\Lambda_s$ .

Unless  $d_i \leq \Lambda_s/2$ , the appropriate value of  $n_i$  is unknown. In fact, many different values of  $n_i$  may satisfy the first inequality. On the other hand, the accuracy of the estimate of  $\phi$  increases with  $d_i$ . To obtain an estimate of  $\phi$  that is both accurate and unambiguous, three or more antennas are used. The first antenna is a reference. The second antenna is separated by  $d_1 \leq \Lambda_s/2$  from the reference. The other antennas are separated by increasingly greater distances from the reference. The first antenna pair provides an unambiguous estimate of the angle of arrival,  $\phi$ . The first and third antennas provide a more accurate estimate of  $\phi$  but an ambiguous one. However, this ambiguity is resolved by the first estimate. Subsequent antennas allow increasingly accurate estimates of  $\phi$ , provided that the ambiguities can be resolved by the less accurate estimates. In designing the interferometer, distance  $d_1$  should correspond to the shortest wavelength to be intercepted.

Assuming that  $n_i$  is correctly determined, the probability density function and moments of  $\hat{\phi}_i$  can be calculated by standard methods once the joint probability density function of  $\hat{\theta}_i$  and  $\hat{\Lambda}_s$  is specified. If there is a negligible error in  $\hat{\Lambda}_s$ , only the probability density function of  $\hat{\theta}_i$  is required. Both of these density functions depend on the details of the receiver implementation.

An alternative method, depicted in figure 21(b), which eliminates the need to estimate  $\Lambda_s$  and the need to resolve ambiguities, is based on the direct measurement of the relative arrival time of a plane wave at two antennas. This relative arrival time can be estimated by using the vector output,  $D_i$ , of the cross correlator in figure 5, or by using two arrival-time estimators.

Assuming that a plane wave is received, the relative arrival time is given by

$$T_r = \frac{d \sin \phi}{v_e}, \quad |\phi| < \frac{\pi}{2}, \quad (172)$$

where  $v_e$  is the speed of electromagnetic waves. Consequently, the angle of arrival estimator is

$$\hat{\phi} = \sin^{-1} \left( \frac{v_e \hat{T}_r}{d} \right), \quad |\hat{\phi}| < \frac{\pi}{2}, \quad (173)$$

where  $\hat{T}_r$  is the relative arrival-time estimator. Retaining the first three terms of a Taylor series expansion of equation (173) about the point  $T_r$  and using equation (172), we obtain

$$\hat{\phi} \approx \phi + \frac{v_e}{d \cos \phi} (\hat{T}_r - T_r) + \frac{v_e^2 \sin \phi}{2d^2 \cos^3 \phi} (\hat{T}_r - T_r)^2, \quad |\phi| < \pi/2, \quad (174)$$

If  $\hat{T}_r$  provides an unbiased estimate of  $T_r$ , then

$$E[\hat{T}_r] = T_r. \quad (175)$$

It follows that

$$E[\hat{\phi}] = \phi + \frac{v_e^2 \sin \phi}{2d^2 \cos^3 \phi} \text{VAR}(\hat{T}_r), \quad |\phi| < \pi/2. \quad (176)$$

Equation (176) shows that the angle estimator is biased even if the arrival-time estimator is unbiased. A straightforward calculation yields the variance of  $\hat{\phi}$ .

The root-mean-square error of  $\hat{\phi}$  is obtained by substituting equation (174) into equation (154). By retaining only the lowest order term, the result is

$$E_R = \frac{v_e}{d \cos \phi} \sigma(\hat{T}_r), \quad |\phi| < \frac{\pi}{2}, \quad (177)$$

where  $\sigma(\hat{T}_r)$  is the standard deviation of  $\hat{T}_r$ . If  $\phi = 0$ ,  $E_R$  has its minimal value. We have

$$E_R = \frac{V_e}{d} \sigma(\hat{T}_r), \quad \phi = 0. \quad (178)$$

This equation indicates that large antenna separations are sometimes necessary if  $E_R$  is to be small. For example, if  $\sigma(\hat{T}_r) = 100$  ns and we desire  $E_R = 0.05$  radians, then we need  $d = 600$  m. However, unless the antenna separation is much smaller than the distance to the source of the intercepted signal, the plane wave assumption and, hence, equation (178) do not apply.

To determine  $\text{VAR}(\hat{T}_r)$ , we must specify the details of the relative arrival-time estimation. For example, if the relative arrival time is computed by subtracting one arrival time from another and if the arrival times are statistically independent with equal variances,  $\text{VAR}(\hat{T}_r)$  is twice the variance of the arrival times. Expressions for the latter variance and various methods for arrival-time estimation can be found in the literature.<sup>13,14</sup>

## 5. CONCLUSIONS

When little is known about a signal to be intercepted, the signal energy and the autocorrelation function present two natural characteristics upon which the interception receiver can base its processing. A radiometer, which measures the signal energy, and a cross correlator, which estimates the autocorrelation function, perform similarly as detectors. The choice between using a radiometer and using a cross correlator is best made on the basis of the additional hardware needed for the receiver's other functions. For example, if a Fourier analysis of the signal and the direction finding with an interferometer are planned, then detection with a cross correlator is preferable since it requires little additional hardware.

A receiver is channelized if its total bandwidth is divided into  $M$  parts by a filter bank, and the filter outputs are processed in parallel. Against narrowband communications, the intercepted power required by a channelized receiver is reduced by a factor of  $\sqrt{M}$  compared with a wideband receiver with the same total bandwidth. Channelized receivers often improve performance against frequency-hopping communications, although a sufficiently high hopping rate may render a channelized design impractical. Pseudonoise spread-spectrum communications require preliminary processing before being applied to a channelized receiver.

<sup>13</sup>B. N. Mityashev, *The Determination of the Time Position of Pulses in the Presence of Noise*, MacDonald, London (1965).

<sup>14</sup>D. J. Torrieri, *Adaptive Thresholding Systems*, *IEEE Trans. Aerosp. Electron. Syst.*, 13 (May 1977), 273.

Channelized receivers, digital filters, acousto-optical devices, and microscan receivers (chirp transform processors) provide comparable resolutions as frequency estimation systems. The systems also theoretically can handle multiple signals that are simultaneously intercepted. The IFM and scanning superheterodyne receivers are less attractive systems in terms of potential capabilities, but may be useful as auxiliary frequency estimators. If speed of frequency estimation is important, it is desirable to use channelized receivers, microscan receivers, or acousto-optical devices with parallel readout of the photodetector outputs. All three systems can provide detection with little additional hardware. In choosing among these three systems, cost and practical implementation problems are among the most important considerations.

If widely separated antennas can be deployed and if the signal to be intercepted has a narrow autocorrelation function, then an interferometer is an effective system for direction finding. Under other circumstances, energy comparison systems and possibly acousto-optical devices are attractive alternatives. Energy comparison systems can be either stationary or rotating. Rotating systems can adjust the antenna position to increase the angle estimation accuracy. When many hostile communications are present, the narrow field of view provides a valuable signal-sorting capability. However, a narrow instantaneous field of view may cause a signal to be missed or may decrease the possible observation time, thereby decreasing the angle estimation accuracy.

By what electronic countermeasures can the communicators thwart interception? The data rates and the transmission powers can be kept to a minimum. Cables and optical fiber links are very helpful whenever feasible. Directional antennas help to conceal the existence of communications from the opponent. However, there are constraints on the degree of directionality that can be designed into an antenna to be used in the battlefield. An important constraint is the need to keep the antenna small to hide it from sight.

Since the antenna beam angle can be decreased by the use of a smaller wavelength as well as by a larger antenna, millimeter or even higher frequencies are sometimes viable alternatives to radio frequencies. The decision to use smaller wavelengths is tempered by such things as cost, available power, and propagation properties. The shorter wavelengths in general are attenuated more than the longer wavelengths and are more easily blocked by obstructions in their path. Furthermore, if the beam width is exceedingly narrow, it is difficult to keep it centered on another station of a communication network.

Time hopping, in which transmissions are increased in total duration, but contain pseudorandom time gaps, is another general countermeasure. Because of the pseudorandom gaps, an interception receiver

must either process more noise energy than it would otherwise or decrease its observation interval. In either case, performance degrades.

Spread-spectrum communications are inherently more difficult to intercept than are conventional communications. Frequency hopping over a wide bandwidth, a powerful countermeasure, complicates the design of an interception receiver and degrades its performance. Detection, frequency-estimation, and direction-finding difficulties increase with the hopping rate.

It is difficult to intercept a signal that is spread over a wide bandwidth. The receiver must process a large amount of noise energy to detect the signal. This is because the signal power is spread over a wide bandwidth, and the receiver must process a large amount of noise energy to detect the signal. This is because the signal power is spread over a wide bandwidth, and the receiver must process a large amount of noise energy to detect the signal.

By not electronic countermeasures can the communication system be intercepted. The data rate and the transmission power can be kept to a minimum. Codes and optical fiber links are very helpful whenever available. Additional knowledge help to detect the existence of communication. However, there are constraints on the amount of bandwidth that can be intercepted and the amount of time that is available. An important constraint is the need to keep the antenna gain as high as possible.

Since the antenna beam width can be decreased by the use of a smaller wavelength as well as by a larger aperture, millimeter or even shorter wavelengths are sometimes used. This is because the antenna gain is proportional to the square of the aperture and inversely proportional to the square of the wavelength. The shorter wavelength is generally not attenuated more than the longer wavelength, and the noise is not usually blocked by obstructions in the path. However, if the beam width is exceedingly narrow, it is difficult to keep it centered on a moving target of a communication network.

The region in which transmission is limited in total duration, but which provides the data, is another general constraint. Because of the bandwidth gap, an interception receiver



#### LITERATURE CITED

- (1) A. Whalen, *Detection of Signals in Noise*, Academic Press, Inc., New York (1971).
- (2) H. L. Van Trees, *Detection, Estimation, and Modulation Theory, III*, John Wiley and Sons, Inc., New York (1971).
- (3) H. Urkowitz, *Energy Detection of Unknown Deterministic Signals*, *Proc. IEEE*, 55 (April 1967), 523.
- (4) R. E. Ziemer and W. H. Tranter, *Systems, Modulation and Noise*, Houghton Mifflin Co., New York (1976).
- (5) A. Papoulis, *Signal Analysis*, McGraw-Hill Book Co., New York (1977).
- (6) R. A. Sprague, *A Review of Acousto-optic Signal Correlators*, *Optical Engineering*, 16 (September 1977), 467.
- (7) D. L. Hecht, *Spectrum Analysis Using Acousto-optic Filters*, *Optical Engineering*, 16 (September 1977), 461.
- (8) R. A. Coppock, R. F. Croce, W. L. Regier, *Bragg Cell RF Signal Processing*, *Microwave J.* (September 1978), 62.
- (9) M. Engelson and F. Telewski, *Spectrum Analyzer Theory and Applications*, Artech House, Inc., Dedham, MA (1974).
- (10) A. A. Oliner, ed., *Acoustic Surface Waves*, Springer-Verlag New York, Inc., New York (1978).
- (11) H. J. Blinchikoff and A. I. Zverev, *Filtering in the Time and Frequency Domains*, John Wiley and Sons, Inc., New York (1976).
- (12) D. K. Barton, *Radar System Analysis*, Artech House, Inc., Dedham, MA (1976).
- (13) B. N. Mityashev, *The Determination of the Time Position of Pulses in the Presence of Noise*, McDonald, London (1965).
- (14) D. J. Torrieri, *Adaptive Thresholding Systems*, *IEEE Trans. Aerosp. Electron. Syst.*, 13 (May 1977), 273.

GLOSSARY OF PRINCIPAL SYMBOLS

$a$	Parameter proportional to bandwidth
$A$	Signal amplitude
$A(t)$	Amplitude modulation
$b$	Measure of beam width
$B$	Bandwidth of filter
$d$	Distance between two antennas
$E$	Signal energy
$E_R$	Root-mean-square error of direction estimate
$E[x]$	Expected value of $x$
$f_c$	Center frequency of filter (hertz)
$f_s$	Frequency of swept local oscillator (hertz)
$f_0$	Carrier frequency of intercepted signal (hertz)
$F(\theta)$	Beam pattern
$h(t)$	Impulse response of filter
$H(\omega)$	Filter transfer function
$I_n(x)$	Modified Bessel function of order $n$
$L$	Receiver output
$m(t)$	Binary message sequence
$M$	Number of channels in channelized radiometer
$n(t)$	White Gaussian noise
$N$	Number of comparator outputs examined during observation interval
$N_0$	Twice noise power spectral density
$N_1$	Number of comparator outputs examined during signal duration
$p(x)$	Probability density function
$P_D$	Probability of detection

64-Blank

GLOSSARY OF PRINCIPAL SYMBOLS (Cont'd)

$P'_D$	Probability that particular radiometer exceeds threshold when signal is present in that radiometer
$P''_D$	Probability that some radiometer exceeds threshold at end of sampling interval when signal is present
$P_F$	Probability of false alarm
$P'_F$	Probability that particular radiometer output exceeds threshold when no signal is present
$r(t)$	Received waveform, usually after bandpass filtering
$R_S$	Received power of intercepted signal
$s(t)$	Signal component
$s'(t)$	Waveform resulting from truncation of $s(t)$
$S(\omega)$	Fourier transform of $s'(t)$
$T$	Observation interval; period of single scan
$T_d$	Duration of impulse response of dispersive filter
$T_r$	Delay in arrival time of intercepted signal at one antenna output relative to arrival time at another output
$T_s$	Duration of sampling interval of channelized radiometer
$T_1$	Signal duration
$v_a$	Acoustic velocity
$v_e$	Electromagnetic velocity
$V$	Test statistic
$V_T$	Fixed threshold level of comparator
$VAR(x)$	Variance of $x$
$W$	Total bandwidth of system (hertz)
$W_S$	Bandwidth of constituent radiometers of channelized radiometer
$\alpha$	Normalized peak value of response of scanning superheterodyne receiver
$\beta$	Parameter defined by equation (4)
$\beta_1$	Parameter defined by equation (44)

GLOSSARY OF PRINCIPAL SYMBOLS (Cont'd)

$\gamma$	Largest integer less than or equal to $TW$
$\delta$	Time delay due to filter or device
$\Delta$	Resolution of frequency estimation system
$\epsilon$	Parameter defined by equation (136)
$\eta$	Largest integer less than or equal to $T_s W_s$
$\theta$	Phase angle; geometrical angle
$\lambda$	Noncentral parameter of chi-square distribution
$\Lambda_a$	Acoustic wavelength
$\Lambda_o$	Optical wavelength
$\Lambda_s$	Signal wavelength
$\mu$	Rate of frequency change (hertz per second)
$\xi$	Parameter defined by equation (5)
$\xi_1$	Parameter defined by equation (45)
$\sigma^2$	Variance
$\phi$	Arrival angle of intercepted signal
$\phi(t)$	Angle modulation function
$\chi^2$	Chi squared, pertaining to probability distribution
$\psi$	Parameter related to maximum of radiation pattern
$\omega_c$	Center frequency of filter (radians per second)
$\omega_s$	Frequency of swept local oscillator (radians per second)
$\omega_0$	Carrier frequency of intercepted signal (radians per second)

DISTRIBUTION

ADMINISTRATOR  
DEFENSE DOCUMENTATION CENTER  
ATTN DDC-TCA (12 COPIES)  
CAMERON STATION, BUILDING 5  
ALEXANDRIA, VA 22314

COMMANDER  
US ARMY MISSILE & MUNITIONS  
CENTER AND SCHOOL  
ATTN ATSK-CTD-F  
REDSTONE ARSENAL, AL 35809

DIRECTOR  
US ARMY MATERIEL SYSTEMS ANALYSIS  
ACTIVITY  
ATTN DRXSY-MP  
ATTN DRXSY-CT  
ABERDEEN PROVING GROUND, MD 21005

DIRECTOR  
DEFENSE ADVANCED RESEARCH PROJECTS  
AGENCY  
ATTN DIR, TACTICAL TECHNOLOGY OFFICE  
ARCHITECT BUILDING  
1400 WILSON BLVD  
ARLINGTON, VA 22209

DIRECTOR  
DEFENSE COMMUNICATIONS ENGINEERING  
CENTER  
ATTN R&D OFFICE, ASST DIR FOR TECH  
1860 WIEHLE AVE  
RESTON, VA 22090

DIRECTOR OF DEFENSE  
RESEARCH & ENGINEERING  
ATTN DEP DIR (TACTICAL WARFARE PROGRAM)  
WASHINGTON, DC 20301

ASSISTANT SECRETARY OF THE ARMY  
(RES, DEV, & ACQ)  
ATTN DEP FOR COMM & TARGET ACQ  
ATTN DEP FOR AIR & MISSILE DEFENSE  
WASHINGTON, DC 20310

COMMANDER  
US ARMY COMMUNICATIONS-ELEC. COMMAND  
ATTN STEEP-MT-M  
FORT HUACHUCA, AZ 85613

OFFICE, DEPUTY CHIEF OF STAFF FOR  
OPERATIONS & PLANS  
DEPARTMENT OF THE ARMY  
ATTN DAMO-TCD, ELECTRONIC/WARFARE  
SIGNAL SECURITY  
ATTN DAMO-RQZ  
WASHINGTON, DC 20310

COMMANDER  
US ARMY CONCEPTS ANALYSIS AGENCY  
8120 WOODMONT AVENUE  
ATTN MDCA-SMS  
BETHESDA, MD 20014

COMMANDER  
US ARMY COMMUNICATIONS R&D COMMAND  
ATTN DRSEL-CE, COMMUNICATIONS-ELECTRONIC  
SYS INTEG OFFICE  
FORT MONMOUTH, NJ 07703

DIRECTOR, ELECTRONIC WARFARE LABORATORY  
ATTN DELEW-V  
ATTN DELEW-C  
ATTN DELEW-E  
ATTN DELEW-M-ST  
FORT MONMOUTH, NJ 07703

COMMANDER  
ELECTRONICS WARFARE LABORATORY  
OFFICE OF MISSILE ELECTRONIC WARFARE  
WHITE SANDS MISSILE RANGE, NM 88002

COMMANDER  
NAVAL WEAPONS CENTER  
ATTN CODE 35, ELECTRONIC WARFARE DEPT  
CHINA LAKE, CA 93555

DIRECTOR  
NAVAL RESEARCH LABORATORY  
ATTN CODE 5700, TACTICAL ELEC  
WARFARE DIVISION  
WASHINGTON, DC 20375

COMMANDER  
NAVAL SURFACE WEAPONS CENTER  
ATTN DF-20, ELECTRONICS WARFARE DIV  
ATTN DK, WARFARE ANALYSIS DEPT  
DAHLGREN, VA 22448

DIRECTOR  
AF AVIONICS LABORATORY  
ATTN KL (WR), ELECTRONIC WARFARE DIV  
WRIGHT-PATTERSON AFB, OH 45433

COMMANDER  
HQ, TACTICAL AIR COMMAND  
ATTN DOR, DIR OF ELECTRONIC  
WARFARE OPNS  
LANGLEY AFB, VA 23665

COMMANDER  
HQ USAF TACTICAL AIR WARFARE  
CENTER (TAC)  
ATTN ER, DCS/ELECTRONIC WARFARE  
AND RECONNAISSANCE  
ATTN ERW, DIR OF ELECTRONIC  
WARFARE  
EGLIN AFB, FL 32542

68-Blank

DISTRIBUTION (Cont'd)

US ARMY ELECTRONICS RESEARCH &  
DEVELOPMENT COMMAND  
ATTN TECHNICAL DIRECTOR, DRDEL-CT  
ATTN DRDEL-CCM (3 COPIES)  
ATTN DRDEL-ST  
ATTN DRDEL-OP  
ATTN TORRIERI, D., DRDEL-CCM (20 COPIES)  
ADELPHI, MD 20783

INSTITUTE FOR DEFENSE ANALYSIS  
400 ARMY NAVY DRIVE  
ARLINGTON, VA 22209

DIA  
DEP DIR OF SCIENTIFIC AND TECH INST  
ELECTRONICS WARFARE BRANCH  
1735 N. LYNN STREET  
ARLINGTON, VA 22209

DEPT OF NAVY  
OFFICE OF RES, DEV, TEST & EVAL  
ATTN TACTICAL AIR SURFACE & EW DEV DIV  
(NOP-982E5)  
ATTN C&C EW AND SENSORS SEC  
(NOP-982F3)  
THE PENTAGON  
WASHINGTON, DC 20350

COMMANDER  
US ARMY TRAINING & DOCTRINE COMMAND  
ATTN ATDC (DCS, COMBAT DEVELOPMENTS)  
FT MONROE, VA 23651

OFFICE OF THE DEPUTY CHIEF OF STAFF  
FOR RES, DEV, & ACQ  
DEPARTMENT OF THE ARMY  
ATTN DAMA-WS  
ATTN DAMA-CS  
ATTN DAMA-AR  
ATTN DAMA-SCS, ELECTRONIC WARFARE TEAM  
WASHINGTON, DC 20310

US ARMY COMBINED ARMS COMBAT DEV ACTIVITY  
ATTN ATZLCA-CA  
ATTN ATZLCA-CO  
ATTN ATZLCA-FS  
ATTN ATZLCA-SW  
ATTN ATZLCA-COM-G  
FT LEAVENWORTH, KS 66027

DIRECTOR  
ELECTRONICS TECHNOLOGY & DEV LAB  
ATTN DELET  
FT MONMOUTH, NJ 07703

COMMANDER  
US ARMY MATERIEL DEV & READINESS COMMAND  
ATTN DRCPP  
ATTN DRCPS  
ATTN DRCDE  
ATTN DRCDE-D  
ATTN DRCBSI  
5001 EISENHOWER AVENUE  
ALEXANDRIA, VA 22333

DIRECTOR  
US ARMY NIGHT VISION AND ELECTRO-OPTICS  
LABORATORY  
FT BELVOIR, VA 22060

COMMANDER  
US ARMY COMBAT SURVEILLANCE AND  
TARGET ACQUISITION LAB  
FT MONMOUTH, NJ 07703

DIRECTOR  
US ARMY SIGNALS WARFARE LAB  
VINT HILL FARMS STATION  
WARRENTON, VA 22186

COMMANDER  
US ARMY INTELLIGENCE AND SECURITY COMMAND  
ARLINGTON HALL STATION  
ATTN IARDA (DCS, RDA)  
ATTN IAITA (DIR, THREAT ANALYSIS)  
4000 ARLINGTON BLVD  
ARLINGTON, VA 22212

US ARMY TRADOC SYSTEMS ANALYSIS  
ACTIVITY  
ATTN ATAA-TDB  
WHITE SANDS MISSILE RANGE, NM 88002

DIRECTOR  
NATIONAL SECURITY AGENCY  
ATTN S65  
FT MEADE, MD 20755

HARRY DIAMOND LABORATORIES  
ATTN 00100, COMMANDER/TECH DIR/TSO  
ATTN CHIEF, 00210  
ATTN CHIEF, 10000  
ATTN CHIEF, 20000  
ATTN CHIEF, 30000  
ATTN CHIEF, 40000  
ATTN RECORD COPY, 81200  
ATTN HDL LIBRARY, 81100 (3 COPIES)  
ATTN HDL LIBRARY, 81100 (WRF)  
ATTN TECHNICAL REPORTS BR, 81300